

ARL 64-23

corrected copy.

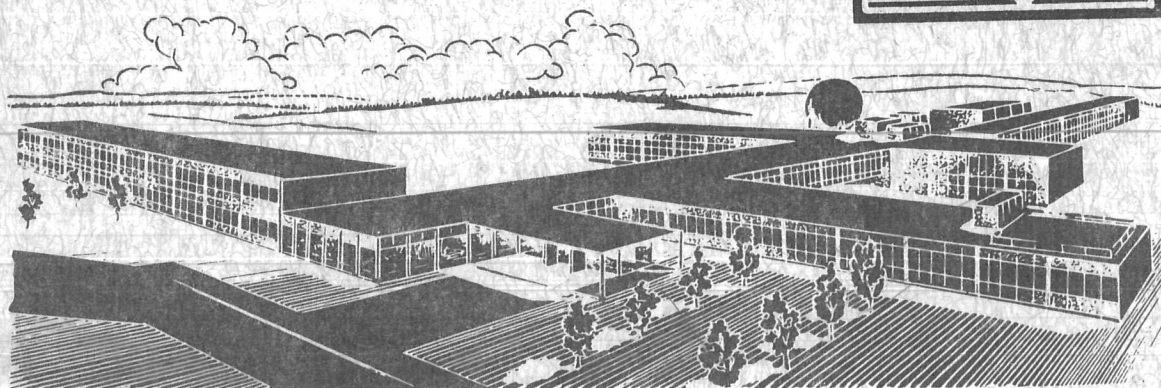
THE STRESSES IN A SPHERICAL SHELL CONTAINING A CRACK

EFTHYMIOS S. FOLIAS

CALIFORNIA INSTITUTE OF TECHNOLOGY
PASADENA, CALIFORNIA

JANUARY 1964

AEROSPACE RESEARCH LABORATORIES
OFFICE OF AEROSPACE RESEARCH
UNITED STATES AIR FORCE



ARL 64-23

**THE STRESSES IN A SPHERICAL SHELL
CONTAINING A CRACK**

EFTHYMIOS S. FOLIAS

*CALIFORNIA INSTITUTE OF TECHNOLOGY
PASADENA, CALIFORNIA*

JANUARY 1964

Contract AF 33(616)-7806
Project 7063
Task 7063-02

AEROSPACE RESEARCH LABORATORIES
OFFICE OF AEROSPACE RESEARCH
UNITED STATES AIR FORCE
WRIGHT-PATTERSON AIR FORCE BASE, OHIO

FOREWORD

This report was prepared by Efthymios S. Foliass of the California Institute of Technology, Pasadena, California. The research reported herein was supported by the Aerospace Research Laboratories, Office of Aerospace Research, United States Air Force on Contract AF 33(616)-7806. The work is documented on Task 7063-02, "Research in the Mechanics of Structures" of Project 7063, "Mechanics of Flight".

The author wishes to express sincere gratitude to Professor M. L. Williams for his inspiring guidance in the preparation of this report and throughout graduate studies. To Professor J. K. Knowles appreciation is extended for his interest and constructive criticism which was a constant source of encouragement. Thanks are due to Professor A. Erdelyi for advice in certain mathematical matters.

Also, thanks are due to Mrs. Elizabeth Fox for the excellent work done in typing the manuscript.

To Drs. Reid Parmerter and Charles D. Babcock, Jr., go thanks for help and suggestions in the experimental work.

ABSTRACT

The deformation of a thin sheet having initial spherical curvature is shown to be associated with that of an initially flat plate resting upon an elastic foundation. Using an integral formulation the coupled Reissner equations for a ~~cracked~~ ^{with a crack} shell of length $2c$ are solved for the in-plane and Kirchhoff bending stresses, and, among other things, it is found that the explicit nature of the stresses near the crack point depends upon the inverse half power of the non-dimensional distance from the point ϵ . The character of the combined extension-bending stress field near the crack tip is investigated in detail for the special case of a radial crack in a spherical cap which is subjected to a uniform internal pressure q_0 and is clamped at the boundary $\bar{R} = \bar{R}_0$. Pending a complete study of the solution, approximate results for the combined surface stresses near the crack tip normal and along the line of crack prolongation are respectively of the form

$$\sigma_y(\epsilon, 0) \Big|_{\nu=1/3} \approx 0.45 \sqrt{\frac{1}{\epsilon}} \frac{q_0 R}{h} + \dots$$

$\lambda = 0.98$
 $c = 0.23 \text{ in}$
 $\bar{R}_0 = 4.25 \text{ in}$

and similarly

$$\sigma_x(\epsilon, 0) \Big|_{\nu=1/3} \approx 0.45 \sqrt{\frac{1}{\epsilon}} \frac{q_0 R}{h} + \dots$$

$\lambda = 0.98$
 $c = 0.23 \text{ in}$
 $\bar{R}_0 = 4.25 \text{ in}$

It is interesting to note that the stresses σ_x and σ_y , along the crack prolongation, for this geometry are equal. In general, they will be of the same sign and will differ only slightly in magnitude due to the bending component. Finally, the experimental and theoretical results for ϵ_y , along the crack prolongation, compare very well.

TABLE OF CONTENTS

CHAPTER	TITLE	PAGE
I	INTRODUCTION	1
II	GENERALITIES	4
III	SPHERICAL SHELL CONTAINING A CRACK	
	3.1 Formulation of the Problem	7
	3.2 Mathematical Statement of the Problem	8
	3.3 Reduction of the System	10
IV	SOLUTION OF THE SYMMETRIC PART	
	4.1 Integral Representation of the Solution	11
	4.2 Boundary and Continuity Conditions in Terms of Integral Representations	11
	4.3 Reduction to Single Integral Equations	13
	4.4 Approximate Integral Equations	18
	4.5 Solution to Approximate Integral Equations for Small λ	19
	4.6 Determination of W and F	23
	4.7 Determination of the Singular Stresses	24
	4.8 Combined Stresses	26
V	SOLUTION OF THE ANTISYMMETRIC PART. INTEGRAL REPRESENTATION. STRESSES	27
VI	PARTICULAR SOLUTION	29
VII	GRIFFITH'S THEORY OF FRACTURE FOR CURVED SHEETS	34
VIII	EXPERIMENTAL VERIFICATION	
	8.1 Description of Experiment	41
	8.2 Preparations	41
	8.3 Conclusions	43

TABLE OF CONTENTS (Cont'd)

CHAPTER	TITLE	PAGE
IX	CONCLUSIONS	44
	APPENDIX I	47
	APPENDIX II	52
	APPENDIX III	61
	REFERENCES	65
	FIGURES	67

NOTATION

c	=	half crack length
D	\equiv	$Eh^3/[12(1-\nu^2)]$ = flexural rigidity
E	=	Young's modulus of elasticity
$F(X, Y)$	=	stress function
G	=	shear modulus
h	=	thickness
h^*		as defined on p. 35 (see fig. 3)
i	\equiv	$\sqrt{-1}$
k	=	$\frac{3-\nu}{1+\nu}$
K_n	=	modified Bessel function of the third kind of order n
l_i	=	kernels as defined in text
l_s	=	$2c$ = crack length of shell
l_p	=	crack length of plate
$(l_{cr})_s$	=	critical crack length of shell
$(l_{cr})_p$	=	critical crack length of plate
L_i^*	=	kernels as defined in text
L_i	\equiv	$\lim_{ y \rightarrow 0} L_i^*$
m_o	=	constant as defined in text
M_x, M_y, M_{xy}	=	moment components
n_o	=	constant as defined in text
N_x, N_y, N_{xy}	=	membrane forces
P	=	periphery
$q(X, Y)$	=	internal pressure
q_o	=	uniform internal pressure
r	=	$\sqrt{x^2+y^2}$

- $r_o \equiv \frac{\bar{R}_o}{c}$
 $R =$ radius of curvature of the shell
 $\bar{R} \equiv \sqrt{X^2 + Y^2}$
 $\bar{R}_o =$ given \bar{R}
 $S =$ surface area of the shell
 $t_o =$ constant as defined in text
 $U =$ energy
 $v_o =$ constant as defined in text
 $V_y =$ equivalent shear
 $W(X, Y) =$ displacement function
 $x, y, z =$ dimensionless coordinates with respect to the crack length
 $X, Y, Z =$ rectangular cartesian coordinates
 $\alpha \equiv (i)^{\frac{1}{2}}$
 $\beta \equiv (-i)^{\frac{1}{2}}$
 $\gamma = 0.5768 =$ Euler's constant
 $\gamma^* =$ surface energy per unit area
 $\delta =$ height of the shell
 $\epsilon \equiv \sqrt{\left(\frac{X-1}{c}\right)^2 + \left(\frac{Y}{c}\right)^2}$
 $\epsilon_x, \epsilon_y, \epsilon_z =$ strain components
 $\zeta \equiv x - \xi$
 $\theta = \tan^{-1} \frac{Y}{X}$
 $\lambda^4 \equiv \frac{Ehc^4}{R^2 D} \equiv \frac{12(1-\nu^2)c^4}{R^2 h^2}$
 $\lambda^* =$ same λ as defined in Appendix II, page 59
 $\nu =$ Poisson's ratio
 $\nu_o \equiv 1 - \nu$

$$\rho \equiv \sqrt{\zeta^2 + y^2} = \sqrt{(x-\xi)^2 + y^2}$$

$\sigma_{x_b}, \sigma_{y_b}, \tau_{xy_b}$ = bending stress components

$\sigma_{x_e}, \sigma_{y_e}, \tau_{xy_e}$ = stretching stress components

$\bar{\sigma}_x, \bar{\sigma}_y, \bar{\tau}_{xy}$ = applied stress components

σ_S^* = critical (fracture) stress for shell

σ_P^* = critical (fracture) stress for plate

$\Phi(x, y), \psi(x, y)$ = harmonic functions

$\chi(x, y)$ = deflection of a plate on an elastic foundation

CHAPTER I
INTRODUCTION

One of the problems in fracture mechanics which apparently has not received extensive theoretical treatment is that concerning the effect of initial curvature upon the stress distribution in a thin sheet containing a crack. Considerable work has been carried out on initially flat sheets subjected to either extensional or bending stresses, and for small deformations the superposition of these separate effects [1] is permissible. On the other hand, if a thin sheet is initially curved, a bending load will generally produce both bending and extensional stresses, and similarly a stretching load will also induce both bending and extensional stresses. The subject of eventual concern therefore is that of the simultaneous stress fields produced in an initially curved sheet containing a crack.

Two geometries immediately come to mind: a spherical shell, and a cylindrical shell. In the latter case one of the principal radii of curvature is infinite and the other constant. It might appear therefore that this geometric simplicity leads to a rather straightforward analytical solution. However, the fact that the curvature varies between zero and a constant as one considers different angular positions — say around the point of a crack which is aligned parallel to the cylinder axis — more than obviates the initial geometric simplification. For this reason a spherical section of a large radius of curvature constant in all directions is chosen for consideration.

It is of some practical value to be able to correlate flat sheet behavior with that of initially curved specimens. In experimental work, for example, considerable time could be saved if a reliable prediction of curved sheet response behavior could be made from flat sheet tests. For this reason an exploratory study was undertaken to assess analytically how the two problems might be related. Although it is recognized that elastic analysis is not directly applicable to fracture prediction because of the plastic flow near the crack tip, considerable information can be obtained.

Chapter II lists the basic assumptions and equations of shallow spherical shells. Then the complementary problem of a cracked spherical shell is formulated in terms of Reissner's shallow shell equations in Chapter III where the problem is separated into two parts, symmetric and antisymmetric. In Chapters IV and V the solutions to the symmetric and antisymmetric parts respectively are expressed in integral form. They are then reduced to the solution of a pair of coupled singular integral equations, which are solved by successive approximations for small values of the characteristic shell parameter $\lambda \equiv \sqrt[4]{12(1-\nu^2)} \frac{c}{\sqrt{Rh}}$. No effort was made to convert the pair of singular integral equations to a corresponding Fredholm type, however Appendix II shows that the two methods are equivalent.

The particular example of a clamped segment of a thin shallow spherical shell is considered in Chapter VI which serves to illustrate how the local solution may be combined in a particular case. Then in Chapter VII, Griffith's criterion is extended to the local region of

an initially spherical curved sheet and an expression for its critical crack length is obtained.

Finally, Chapter VIII compares the experimental and theoretical results for the particular problem described in Chapter VI.

CHAPTER II
GENERALITIES

In the following, we consider bending and stretching of thin shells of revolution, as described by traditional two-dimensional linear theory, with the additional assumption of shallowness. In speaking of the formulation of two-dimensional differential equations, we mean the transition from the exact three-dimensional elasticity problem to that of two-dimensional approximate formulation, which is appropriate in view of the "thinness" of the shell. In this paper, we limit ourselves to isotropic and homogeneous shallow segments* of elastic spherical shells of constant thickness. It is also assumed that the shell is subjected to small deformations and strains so that the stress-strain relations may be established through Hooke's law.

The basic variables in the theory of shallow shells are the displacement component $W(X,Y)$ in the direction of an axis Z , which for shells of revolution coincides with the axis of symmetry of the shell, and a stress function $F(X,Y)$ which represents the stress resultants tangent to the middle surface of the shell. Following Reissner [2], the coupled differential equations governing W and F , with X and Y as rectangular coordinates of the base plane (see fig. 1), are given by:

$$-\frac{Eh}{R} \nabla^2 W(x,y) + \nabla^4 F(x,y) = 0 \quad (2.1)$$

$$\nabla^4 W(x,y) + \frac{1}{Rb} \nabla^2 F(x,y) = \frac{q(x,y)}{b} \quad (2.2)$$

* A segment will be called shallow if the ratio of height to base diameter is less than, say, 1/8.

The usual bending moment components M_x , M_y , M_{xy} are defined in terms of the displacement function W as:

$$M_x = -D \left[\frac{\partial^2}{\partial X^2} + \nu \frac{\partial^2}{\partial Y^2} \right] W \quad (2.3)$$

$$M_y = -D \left[\frac{\partial^2}{\partial Y^2} + \nu \frac{\partial^2}{\partial X^2} \right] W \quad (2.4)$$

$$M_{xy} = -D(1-\nu) \frac{\partial^2 W}{\partial X \partial Y} \quad (2.5)$$

Similarly, the membrane forces are defined in terms of the stress function F as:

$$N_x = \frac{\partial^2 F}{\partial Y^2} \quad (2.6)$$

$$N_y = \frac{\partial^2 F}{\partial X^2} \quad (2.7)$$

$$N_{xy} = - \frac{\partial^2 F}{\partial X \partial Y} \quad (2.8)$$

In view of (2.3) - (2.8) the bending stress components are

$$\sigma_{x_b} = - \frac{E Z}{(1-\nu^2)} \left[\frac{\partial^2 W}{\partial X^2} + \nu \frac{\partial^2 W}{\partial Y^2} \right] \quad (2.9)$$

$$\sigma_{y_b} = - \frac{E Z}{(1-\nu^2)} \left[\frac{\partial^2 W}{\partial Y^2} + \nu \frac{\partial^2 W}{\partial X^2} \right] \quad (2.10)$$

$$\tau_{xy_b} = - 2 G Z \frac{\partial^2 W}{\partial X \partial Y} \quad (2.11)$$

Similarly, the extensional stress components are

$$\sigma_{x_e} = \frac{1}{h} \frac{\partial^2 F}{\partial Y^2} \quad (2.12)$$

$$\sigma_{y_e} = \frac{1}{h} \frac{\partial^2 F}{\partial X^2} \quad (2.13)$$

$$\tau_{xy_e} = -\frac{1}{h} \frac{\partial^2 F}{\partial X \partial Y} \quad (2.14)$$

CHAPTER III

CRACKED SPHERICAL SHELL

1. Formulation of the Problem

Consider a portion of a thin, shallow spherical shell of constant thickness h and subjected to an internal pressure $q(X,Y)$. The material of the shell is assumed to be homogeneous and isotropic and at the apex there exists a radial cut of length $2c$ with respect to the apex. The coupled differential equations governing the bending deflection $W(X, Y)$ and membrane stress function $F(X, Y)$ are given by 2.1 and 2.2. It is convenient at this point to introduce dimensionless coordinates, namely

$$x \equiv \frac{X}{c}, \quad y \equiv \frac{Y}{c} \quad (3.1)$$

which change the homogeneous parts of ~~1.1~~^{2.1} and ~~1.2~~^{2.2} to:

$$-\frac{Eh^3c^2}{R} \nabla^2 W + \nabla^4 F = 0 \quad (3.2)$$

$$\nabla^4 W + \frac{c^2}{R\Delta} \nabla^2 F = 0 \quad (3.3)$$

As to boundary conditions, one must now require that the normal moment, equivalent vertical shear, and normal and tangential in-plane stresses vanish along the crack. However, suppose that one has already found* a particular solution satisfying 3.2 and 3.3, but that there is a residual normal moment M_y , equivalent vertical shear V_y , normal in-plane stress N_y , and an in-plane tangential stress N_{xy} , along the real axis $|x| < 1$, of the form:

* See particular solution, Chapter VI.

$$M_y^{(P)} = - \frac{D}{c^2} m_o \quad (3.4)$$

$$V_y^{(P)} = - \frac{D}{c^2} v_o \quad (3.5)$$

$$N_y^{(P)} = - \frac{n_o}{c^2} \quad (3.6)$$

$$N_{xy}^{(P)} = - \frac{t_o}{c^2} \quad (3.7)$$

For simplicity, we take m_o, v_o, n_o, t_o to be constants* and furthermore we divide the problem into two parts:

Symmetrical: where $v_o = t_o = 0$

Antisymmetrical: where $m_o = n_o = 0$

2. Mathematical Statement of the Problem

Assuming therefore that a particular solution has been found, we need to find now two functions of the dimensionless coordinates (x, y) , $W(x, y)$ and $F(x, y)$, such that they satisfy the partial differential equations:

$$- \frac{ERc^2}{R} \nabla^2 W + \nabla^4 F = 0 \quad (3.2)$$

$$\nabla^4 W + \frac{c^2}{RD} \nabla^2 F = 0 \quad (3.3)$$

* For m_o, n_o, t_o, v_o non-constants, see the remarks on Chapter IV, section 7.

and the following boundary conditions. At $y = 0$ and $|x| < 1$:

$$M_y(x,0) = -\frac{D}{c^2} \left[\frac{\partial^2 w}{\partial y^2} + \nu \frac{\partial^2 w}{\partial x^2} \right] = \frac{D m_0}{c^2} \quad (3.8)$$

$$V_y(x,0) = -\frac{D}{c^3} \left[\frac{\partial^3 w}{\partial y^3} + (2-\nu) \frac{\partial^3 w}{\partial x^2 \partial y} \right] = D \frac{v_0}{c^3} \quad (3.9)$$

$$N_y(x,0) = \frac{1}{c^2} \frac{\partial^2 F}{\partial x^2} = \frac{n_0}{c^2} \quad (3.10)$$

$$N_{xy}(x,0) = -\frac{1}{c^2} \frac{\partial^2 F}{\partial x \partial y} = \frac{t_0}{c^2} \quad (3.11)$$

Next, to satisfy continuity requirements, we require the following equations to hold for $y = 0$ and $|x| > 1$

$$\lim_{|y| \rightarrow 0} \left[\frac{\partial^\eta}{\partial y^\eta} (w^+) - \frac{\partial^\eta}{\partial y^\eta} (w^-) \right] = 0 \quad (3.12)$$

$$\lim_{|y| \rightarrow 0} \left[\frac{\partial^\eta}{\partial y^\eta} (F^+) - \frac{\partial^\eta}{\partial y^\eta} (F^-) \right] = 0 \quad (3.13)$$

($\eta = 0, 1, 2, 3.$)

Furthermore, because we are limiting ourselves to a large radius of curvature for this shallow shell, i. e., small deviations from a flat sheet, we can apply certain boundary conditions at infinity even though we know physically that the stresses and displacements far away from the crack are finite. Therefore, to avoid infinite stresses and infinite displacements we must require that the displacement function W and the stress function F with their first derivatives to be finite far away from the crack. These restrictions simplify the mathematical

complexities of the problem considerably, and correspond to the usual expectations of the St. Venant Principle. It should be pointed out that the boundary conditions at infinity are not geometrically feasible. However if the crack is small compared to the dimensions of the shell, the approximation is good.

3. Reduction of the System

Reissner [3] has shown that the solution to the system (3.2), (3.3) can be written in the form

$$W = \chi + \Phi \quad (3.14)$$

$$F = -\frac{RD}{c^2} \nabla^2 \chi + \psi \quad (3.15)$$

where Φ and ψ are harmonic functions and χ satisfies the same differential equation as the deflection of a plate on an elastic foundation, i. e.,

$$(\nabla^4 + \lambda^4) \chi = 0 \quad (3.16)$$

where

$$\lambda^4 \equiv \frac{ERc^4}{R^2D} \equiv \frac{12(1-\nu^2)}{(R/h)^2} \left(\frac{c}{h}\right)^4 \quad (3.17)$$

The function ψ represents the inextensional bending part of the solution, and Φ represents the membrane part of the solution.

CHAPTER IV

SOLUTION OF THE SYMMETRIC PART

1. Integral Representations of the Solution

We next construct the following representations which have the proper symmetrical behavior with respect to x ,

$$W(x, y^\pm) = \int_0^\infty \left\{ P_1 e^{-\sqrt{s^2 - i\lambda^2}|y|} + P_2 e^{-\sqrt{s^2 + i\lambda^2}|y|} + P_3 e^{-s|y|} \right\} \cos xs ds \quad (4.1)$$

$$F(x, y^\pm) = \frac{i\lambda^2 R D}{c^2} \int_0^\infty \left\{ P_1 e^{-\sqrt{s^2 - i\lambda^2}|y|} - P_2 e^{-\sqrt{s^2 + i\lambda^2}|y|} + P_4 e^{-s|y|} \right\} \cos xs ds \quad (4.2)$$

where the P_i 's ($i = 1, 2, 3, 4$) are arbitrary functions of s to be determined from the boundary conditions, and the \pm signs refer to $y > 0$ and $y < 0$ respectively.

2. The Boundary and Continuity Conditions in Terms of the Integral Representation

Assuming that we can differentiate under the integral sign, formally substituting 4.2 into 3.10, 3.11 yields respectively:

$$\lim_{|y| \rightarrow 0} \left\{ -\frac{i\lambda^2 R D}{c^2} \int_0^\infty \left[P_1 e^{-\sqrt{s^2 - i\lambda^2}|y|} - P_2 e^{-\sqrt{s^2 + i\lambda^2}|y|} + P_4 e^{-s|y|} \right] s^2 \cos xs ds \right\} = \eta_0 ; |x| < 1 \quad (4.3)$$

and

$$\lim_{|y| \rightarrow 0} \left\{ \mp \frac{i\lambda^2 R D}{c^2} \int_0^\infty \left[P_1 \sqrt{s^2 - i\lambda^2} e^{-\sqrt{s^2 - i\lambda^2}|y|} - P_2 \sqrt{s^2 + i\lambda^2} e^{-\sqrt{s^2 + i\lambda^2}|y|} + P_4 s e^{-s|y|} \right] s \sin xs ds \right\} = 0 \quad (4.4)$$

where again the $\bar{\tau}$ signs refer to $y > 0$ and $y < 0$ respectively. A sufficient condition for Eq. 4.4 to be satisfied is to set

$$s P_4 = - (P_1 \sqrt{s^2 - i\lambda^2} - P_2 \sqrt{s^2 + i\lambda^2}) \quad (4.5)$$

Furthermore, it can be shown that the continuity conditions on F and its derivatives for $y = 0$ and $|x| > 1$ are satisfied if we take

$$\int_0^{\infty} \{ \sqrt{s^2 - i\lambda^2} P_1 + \sqrt{s^2 + i\lambda^2} P_2 \} \cos xs \, ds = 0 \quad ; \quad |x| > 1 \quad (4.6)$$

Similarly, introducing 4.2 into 3.8 and 3.9 we obtain respectively:

$$\lim_{|y| \rightarrow 0} \left\{ \int_0^{\infty} \left[P_1 (\nu_0 s^2 - i\lambda^2) e^{-\sqrt{s^2 - i\lambda^2} |y|} + P_2 (\nu_0 s^2 + i\lambda^2) e^{-\sqrt{s^2 + i\lambda^2} |y|} + \nu_0 s^2 P_3 e^{-s|y|} \right] \cos xs \, ds \right\} = -m_0 \quad ; \quad |x| < 1 \quad (4.7)$$

and

$$\lim_{|y| \rightarrow 0} \left\{ \pm \int_0^{\infty} \left[P_1 \sqrt{s^2 - i\lambda^2} (\nu_0 s^2 + i\lambda^2) e^{-\sqrt{s^2 - i\lambda^2} |y|} + P_2 \sqrt{s^2 + i\lambda^2} (\nu_0 s^2 - i\lambda^2) e^{-\sqrt{s^2 + i\lambda^2} |y|} + \nu_0 s^3 P_3 e^{-s|y|} \right] \cos xs \, ds \right\} = 0 \quad ; \quad |x| < 1 \quad (4.8)$$

Again, a sufficient condition for Eq. 4.8 is to take

$$\nu_0 s^3 P_3 = - \left\{ \sqrt{s^2 - i\lambda^2} (\nu_0 s^2 + i\lambda^2) P_1 + \sqrt{s^2 + i\lambda^2} (\nu_0 s^2 - i\lambda^2) P_2 \right\} \quad (4.9)$$

Further it may be easily shown that the continuity conditions are satisfied if

$$\int_0^{\infty} \left\{ \sqrt{s^2 - i\lambda^2} P_1 - \sqrt{s^2 + i\lambda^2} P_2 \right\} \frac{1}{s^2} \cos xs \, ds = 0 \quad ; \quad |x| > 1 \quad (4.10)$$

In view of 4.6 and 4.10 we conclude that the individual integrals must vanish, namely

$$\int_0^{\infty} \frac{P_1}{s^2} \sqrt{s^2 - i\lambda^2} \cos xs \, ds = 0 \quad ; \quad |x| > 1 \quad (4.11)$$

$$\int_0^{\infty} \frac{P_2}{s^2} \sqrt{s^2 - i\lambda^2} \cos xs \, ds = 0 \quad ; \quad |x| > 1 \quad (4.12)$$

Therefore we have reduced our problem to solving the dual integral equations 4.3, 4.7, 4.11 and 4.12 for the unknown functions $P_1(s)$ and $P_2(s)$.

3. Reduction to Single Integral Equations

Because we are unable to solve dual integral equations of the type discussed in the previous section, therefore we will reduce the problem to singular integral equations. Let

$$u_1(x) = \int_0^{\infty} \frac{P_1}{s^2} \sqrt{s^2 - i\lambda^2} \cos xs \, ds \quad ; \quad |x| < 1 \quad (4.13)$$

and

$$u_2(x) = \int_0^{\infty} \frac{P_2}{s^2} \sqrt{s^2 + i\lambda^2} \cos xs \, ds \quad ; \quad |x| < 1 \quad (4.13a)$$

which by Fourier inversion gives:

$$\frac{P_1(s)}{s^2} \sqrt{s^2 - i\lambda^2} = \frac{2}{\pi} \int_0^{\infty} u_1(\xi) \cos \xi s \, d\xi \quad (2.31)$$

and solving for P_1

$$P_1(s) = \frac{2}{\pi} \frac{s^2}{\sqrt{s^2 - i\lambda^2}} \int_0^{\infty} u_1(\xi) \cos \xi s \, d\xi \quad (4.14)$$

Similarly

$$P_2(s) = \frac{2}{\pi} \frac{s^2}{\sqrt{s^2 + i\lambda^2}} \int_0^1 u_2(\xi) \cos \xi s d\xi \quad (4.15)$$

where the functions $u_1(\xi)$ and $u_2(\xi)$, due to the symmetry of the problem, are even. Formally substituting 4.14 and 4.15 into 4.3, 4.7 we find after changing the order of integration and rearranging

$$N_y = -\frac{2i\lambda^2 R D}{\pi c^2} \int_{-1}^1 \left\{ u_1(\xi) L_1^* - u_2(\xi) L_2^* \right\} d\xi \quad (4.16)$$

$$M_y = -\frac{2D}{\pi} \int_{-1}^1 \left\{ u_1(\xi) L_3^* + u_2(\xi) L_4^* \right\} d\xi \quad (4.17)$$

where

$$L_1^* = \frac{1}{2} \int_0^\infty \frac{s^4}{\sqrt{s^2 - \alpha^2 \lambda^2}} e^{-\sqrt{s^2 - \alpha^2 \lambda^2} |y|} \cos(x-\xi) s ds - \frac{1}{2} \int_0^\infty s^3 e^{-s|y|} \cos(x-\xi) s ds \quad (4.18)$$

$$L_2^* = \frac{1}{2} \int_0^\infty \frac{s^4}{\sqrt{s^2 - \beta^2 \lambda^2}} e^{-\sqrt{s^2 - \beta^2 \lambda^2} |y|} \cos(x-\xi) s ds - \frac{1}{2} \int_0^\infty s^3 e^{-s|y|} \cos(x-\xi) s ds \quad (4.19)$$

$$L_3^* = \frac{1}{2} \int_0^\infty \left\{ \frac{s^2 (\gamma_0 s^2 + i\lambda^2)}{\sqrt{s^2 - \alpha^2 \lambda^2}} e^{-\sqrt{s^2 - \alpha^2 \lambda^2} |y|} - s (\gamma_0 s^2 + i\lambda^2) e^{-s|y|} \right\} \cos(x-\xi) s ds \quad (4.20)$$

$$L_4^* = \frac{1}{2} \int_0^\infty \left\{ \frac{s^2 (\gamma_0 s^2 + i\lambda^2)}{\sqrt{s^2 - \beta^2 \lambda^2}} e^{-\sqrt{s^2 - \beta^2 \lambda^2} |y|} - s (\gamma_0 s^2 + i\lambda^2) e^{-s|y|} \right\} \cos(x-\xi) s ds \quad (4.21)$$

The integrations in 4.18-4.21 may be carried out explicitly by making use of the Fourier cosine transforms*

$$\int_0^{\infty} e^{-\lambda|s|} \cos \zeta s ds = \frac{|\lambda|}{\rho^2} \quad (4.22)$$

$$\int_0^{\infty} \frac{e^{-\sqrt{s^2+a^2}|\lambda|}}{\sqrt{s^2+a^2}} \cos \zeta s ds = K_0(a\rho) ; \operatorname{Re} a > 0 \quad (4.23)$$

and similar results obtained by differentiating them with respect to x and y (see Appendix I). In these formulas $\rho^2 = \zeta^2 + y^2$, and K_n denotes the modified Bessel function of the third kind of order n .

The expressions 4.18-4.21 then become respectively

$$2L_1^* \equiv \frac{\partial}{\partial x} \left\{ -\frac{\lambda^2 \zeta}{\rho^4} (\zeta^2 - 3y^2) K_0(\lambda \rho e) - \left[\frac{\lambda^3 \rho^3 \zeta^3}{\rho^3} + \frac{2\lambda \rho \zeta}{\rho^5} (\zeta^2 - 3y^2) \right] K_1(\lambda \rho e) + \frac{2\zeta}{\rho^4} - \frac{8\zeta |y|^2}{\rho^6} \right\} \quad (4.24)$$

$$2L_2^* \equiv \frac{\partial}{\partial x} \left\{ -\frac{\lambda^2 \alpha^2 \zeta}{\rho^4} (\zeta^2 - 3|y|^2) K_0(\lambda \alpha \rho) - \left[\frac{\lambda^3 \alpha^3 \zeta^3}{\rho^3} + \frac{2\lambda \alpha \zeta}{\rho^5} (\zeta^2 - 3|y|^2) \right] K_1(\lambda \alpha \rho) + \frac{2\zeta}{\rho^4} - \frac{8\zeta |y|^2}{\rho^6} \right\} \quad (4.25)$$

$$2L_3^* \equiv \frac{\partial}{\partial x} \left\{ -\frac{\lambda_0 \lambda^2 \rho^2 \zeta}{\rho^4} (\zeta^2 - 3|y|^2) K_0(\lambda \rho e) - \lambda_0 \left[\frac{\lambda^3 \rho^3 \zeta^3}{\rho^3} + \frac{2\lambda \rho \zeta}{\rho^5} (\zeta^2 - 3|y|^2) \right] K_1(\lambda \rho e) - \frac{\alpha^2 \lambda^3 \rho \zeta}{\rho} K_1(\lambda \rho e) + \frac{2\lambda_0 \zeta}{\rho^4} - \frac{8\zeta |y|^2 \lambda_0}{\rho^6} - \frac{\alpha^2 \lambda^2 \zeta}{\rho^2} \right\} \quad (4.26)$$

* Formulas 4.22 and 4.23 may be obtained from [4], pages 14 and 17 respectively.

$$2L_4^* \equiv \frac{\partial}{\partial x} \left\{ -\frac{\nu_0 \lambda^2 \alpha^2 \zeta}{\rho^4} (\zeta^2 - 3|y|^2) K_0(\lambda \alpha \rho) - \nu_0 \left[\frac{\lambda^3 \alpha^3 \zeta^3}{\rho^3} + \frac{2\lambda \alpha \zeta}{\rho^5} (\zeta^2 - 3|y|^2) \right] K_1(\lambda \alpha \rho) \right. \\ \left. - \frac{\beta^2 \lambda^3 \alpha \zeta}{\rho} K_1(\lambda \alpha \rho) + \frac{2\nu_0 \zeta}{\rho^4} - \frac{8\zeta |y|^2 \nu_0}{\rho^6} - \frac{\rho^2 \lambda^2 \zeta}{\rho^2} \right\} \quad (4.27)$$

Thus, the limits as $|y| \rightarrow 0$ of N_y and M_y are found to be respectively

$$\lim_{|y| \rightarrow 0} N_y = -\frac{2i\lambda^2 R D}{\pi c^2} \frac{d}{dx} \int_{-1}^1 \left\{ u_1(\xi) L_1 - u_2(\xi) L_2 \right\} d\xi$$

$$\lim_{|y| \rightarrow 0} M_y = -\frac{2D}{\pi} \frac{d}{dx} \int_{-1}^1 \left\{ u_1(\xi) L_3 + u_2(\xi) L_4 \right\} d\xi$$

where the integrals are understood to be of Cauchy principal value and

$$2L_1 \equiv -\frac{\lambda^2 \beta^2}{\zeta} K_0(\lambda \rho |\zeta|) - \left(\lambda^3 \rho^3 \frac{\zeta}{|\zeta|} + \frac{2\lambda \rho}{\zeta |\zeta|} \right) K_1(\lambda \rho |\zeta|) + \frac{2}{\zeta^3} \quad (4.28)$$

$$2L_2 \equiv -\frac{\lambda^2 \alpha^2}{\zeta} \left(K_0(\lambda \alpha |\zeta|) - \left(\lambda^3 \alpha^3 \frac{\zeta}{|\zeta|} + \frac{2\lambda \alpha}{\zeta |\zeta|} \right) K_1(\lambda \alpha |\zeta|) \right) + \frac{2}{\zeta^3} \quad (4.29)$$

$$2L_3 \equiv -\frac{\nu_0 \lambda^2 \beta^2}{\zeta} \left(K_0(\lambda \rho |\zeta|) - \nu_0 \left(\lambda^3 \rho^3 \frac{\zeta}{|\zeta|} + \frac{2\lambda \rho}{\zeta |\zeta|} \right) K_1(\lambda \rho |\zeta|) \right) + \\ -\alpha^2 \lambda^3 \beta \frac{\zeta}{|\zeta|} K_1(\lambda \rho |\zeta|) + \frac{2\nu_0}{\zeta^3} - \frac{\alpha^2 \lambda^2}{\zeta} \quad (4.30)$$

$$2L_4 \equiv -\frac{\nu_0 \lambda^2 \alpha^2}{\zeta} \left(K_0(\lambda \alpha |\zeta|) - \nu_0 \left(\lambda^3 \alpha^3 \frac{\zeta}{|\zeta|} + \frac{2\lambda \alpha}{\zeta |\zeta|} \right) K_1(\lambda \alpha |\zeta|) \right) + \\ -\beta^2 \lambda^3 \alpha \frac{\zeta}{|\zeta|} K_1(\lambda \alpha |\zeta|) + \frac{2\nu_0}{\zeta^3} - \frac{\beta^2 \lambda^2}{\zeta} \quad (4.31)$$

If we set N_y, M_y , in the limit as $|y| \rightarrow 0$, equal to $-n_0$ and $-m_0$ respectively, integrate with respect to x , then we find that they must satisfy the integral equations

$$\int_{-1}^1 \{ u_1(\xi) 2L_1 - u_2(\xi) 2L_2 \} d\xi = -\frac{\pi n_0 c^2}{l \lambda^2 R D} x \quad ; \quad |x| < 1 \quad (4.32)$$

$$\int_{-1}^1 \{ u_1(\xi) 2L_3 + u_2(\xi) 2L_4 \} d\xi = -\pi m_0 x \quad ; \quad |x| < 1 \quad (4.33)$$

The kernels L_1, L_2, L_3, L_4 have singularities of the order $\frac{1}{\zeta} \equiv \frac{1}{x-\xi}$, as can easily be seen by observing their behavior for small arguments: *

$$\begin{aligned} 2L_1 = & -\frac{\lambda^2 \beta^2}{2(x-\xi)} + \lambda^4 \beta^4 (x-\xi) \left[\frac{5}{32} - \frac{3\gamma}{8} - \frac{3}{8} \ln \lambda \beta \frac{|x-\xi|}{2} \right] \\ & \lambda^6 \beta^6 (x-\xi)^3 \left[\frac{7}{128} - \frac{3\gamma}{64} - \frac{3}{64} \ln \lambda \beta \frac{|x-\xi|}{2} \right] \\ & + O(\lambda^6 (x-\xi)^3 \ln \lambda |x-\xi|) \end{aligned} \quad (4.34)$$

$$\begin{aligned} 2L_2 = & -\frac{\lambda^2 \alpha^2}{2(x-\xi)} + \lambda^4 \alpha^4 (x-\xi) \left[\frac{5}{32} - \frac{3\gamma}{8} - \frac{3}{8} \ln \lambda \alpha \frac{|x-\xi|}{2} \right] \\ & \lambda^6 \alpha^6 (x-\xi)^3 \left[\frac{7}{128} - \frac{3\gamma}{64} - \frac{3}{64} \ln \lambda \alpha \frac{|x-\xi|}{2} \right] \\ & + O(\lambda^6 (x-\xi)^3 \ln \lambda |x-\xi|) \end{aligned} \quad (4.35)$$

$$\begin{aligned} 2L_3 = & -\frac{\lambda^2 \alpha^2 (4-\nu_0)}{2(x-\xi)} + \lambda^4 \beta^4 (x-\xi) \left[\frac{5\nu_0-8}{32} + \frac{4-3\nu_0}{8} (\gamma + \ln \lambda \beta \frac{|x-\xi|}{2}) \right] \\ & \lambda^6 \beta^6 (x-\xi)^3 \left[\frac{7\nu_0-10}{128} + \frac{4-3\nu_0}{64} (\gamma + \ln \lambda \beta \frac{|x-\xi|}{2}) \right] \\ & + O(\lambda^6 (x-\xi)^3 \ln \lambda |x-\xi|). \end{aligned} \quad (4.36)$$

* See Appendix I for expansions of $K_n(z)$ for small z .

$$\begin{aligned}
 2L_4 = & -\frac{\lambda^2 \beta^2 (4-\nu_0)}{2(x-\xi)} + \lambda^2 \alpha^2 (x-\xi) \left[\frac{5\nu_0-8}{32} + \frac{4-3\nu_0}{8} (\gamma + \ln \lambda \frac{|x-\xi|}{2}) \right] \\
 & \lambda^6 \alpha^6 (x-\xi) \left[\frac{7\nu_0-10}{128} + \frac{4-3\nu_0}{64} (\gamma + \ln \lambda \frac{|x-\xi|}{2}) \right] \\
 & + O(\lambda^6 (x-\xi)^3 \ln \lambda |x-\xi|)
 \end{aligned} \tag{4.37}$$

We require that the solutions $u_1(x)$, $u_2(x)$ be Hölder continuous for some positive Hölder indices μ_1 and μ_2 for all x in the closed interval $[-1,1]$. Thus in particular $u_1(x)$, $u_2(x)$ are to be bounded near the ends of the crack.

The problem of obtaining a solution to the coupled integral equations 4.32 and 4.33 can be reduced to the problem of solving two coupled Fredholm integral equations with a bounded kernel. See Appendix II.

4. Approximate Integral Equations

Because of the complicated nature of the kernels L_1 , L_2 , L_3 and L_4 , an exact solution for the unknown functions $u_1(x)$ and $u_2(x)$ is extremely difficult. On the other hand, for most practical applications the parameter λ attains small values as follows from the definition of λ namely

$$\lambda \equiv \frac{\sqrt[4]{12(1-\nu^2)}}{\sqrt{R/h}} \quad (c/h) = \sqrt[4]{12(1-\nu^2)} \quad (c/R) \cdot \left(\frac{R}{h}\right)^{1/2}$$

It is clear that λ is small for large ratios of $\frac{R}{h}$ and small crack lengths. As a practical matter, if we consider crack lengths less than one tenth of the periphery, i.e. $2c < \frac{2\pi R}{10}$, and for $\frac{R}{h} < 10^3$ a corresponding upper bound for λ can be obtained, namely $\lambda < 20$. Thus the range of

λ becomes $0 < \lambda < 20$ and for most practical cases is between 0 and 2, depending upon the size of the crack.

If we consider small λ , we may replace the exact singular integral equations with the following approximate set

$$\int_{-1}^1 \{ u_{10}(\xi) z l_1 - u_{20}(\xi) z l_2 \} d\xi = - \frac{n_0 c^2 \pi}{i \lambda^2 R D} x \quad ; \quad |x| < 1 \quad (4-38)$$

$$\int_{-1}^1 \{ u_{10}(\xi) z l_3 + u_{20}(\xi) z l_4 \} d\xi = - m_0 \pi x \quad ; \quad |x| < 1 \quad (4.39)$$

where the new kernels are:

$$z l_1 = - \frac{\lambda^2 \beta^2}{2(x-\xi)} + \lambda^4 \beta^4 (x-\xi) \left[\frac{5}{32} - \frac{3x}{8} - \frac{3}{8} \ln \frac{\lambda \beta |x-\xi|}{2} \right] \quad (4.40)$$

$$z l_2 = - \frac{\lambda^2 \alpha^2}{2(x-\xi)} + \lambda^4 \alpha^4 (x-\xi) \left[\frac{5}{32} - \frac{3x}{8} - \frac{3}{8} \ln \frac{\lambda \alpha |x-\xi|}{2} \right] \quad (4.41)$$

$$z l_3 = - \frac{\alpha^2 \lambda^2 (4-\nu_0)}{2(x-\xi)} + \lambda^4 \alpha^4 (x-\xi) \left[\frac{5\nu_0-8}{32} + \frac{4-3\nu_0}{8} \left(\gamma + \ln \frac{\lambda \beta |x-\xi|}{2} \right) \right] \quad (4.42)$$

$$z l_4 = - \frac{\beta^2 \lambda^2 (4-\nu_0)}{2(x-\xi)} + \lambda^4 \beta^4 (x-\xi) \left[\frac{5\nu_0-8}{32} + \frac{4-3\nu_0}{8} \left(\gamma + \ln \frac{\lambda \alpha |x-\xi|}{2} \right) \right] \quad (4.43)$$

5. Solution to Approximate Integral Equations for Small λ

For the simple case $\lambda = 0$ the problem reduces to that of a flat sheet under applied bending and stretching loads, the solution of which

has been investigated by many authors. For example, the problem for both bending and stretching for an orthotropic plate, containing a finite crack, was investigated by Ang and Williams [1] and a solution was obtained by means of dual integral equations. It can easily be shown* that the dual integral equations can be transformed to two singular integral equations of the type 4.32 and 4.33 with simpler kernels. Furthermore, these are not coupled and the solutions can easily be obtained as in §47 of [6]. Without going into the details they are found to be of the form $A\sqrt{1-\xi^2}$, where A is a constant.

Similarly, the solution for an initially curved sheet must, in the limit, check the above result and because $u_1(\xi)$ and $u_2(\xi)$ are in particular to be bounded near the ends of the crack, it is reasonable to assume solutions of the form

$$u_{10}(\xi) = \sqrt{1-\xi^2} \left[A_1 + \lambda^2 A_2 (1-\xi^2) + \dots \right] \quad ; |\xi| < 1 \quad (4.44)$$

$$u_{20}(\xi) = \sqrt{1-\xi^2} \left[B_1 + \lambda^2 B_2 (1-\xi^2) + \dots \right] \quad ; |\xi| < 1 \quad (4.45)$$

where the coefficients $A_1, A_2, \dots, B_1, B_2, \dots$ can be functions of λ but not of ξ .

Substituting 4.44 and 4.45 into 4.38 and 4.39 and making use of the integrals given in Appendix I we obtain:

* See Noble [5].

$$\begin{aligned}
 & A_1 \left\{ -\frac{\lambda^2 \beta^2}{2} \pi x + \lambda^4 \beta^4 \left(\frac{5}{32} - \frac{3\gamma}{8} \right) \frac{\pi}{2} x - \frac{3}{8} \lambda^4 \beta^4 \left[\frac{\pi}{4} \left(1 + \ln \frac{\lambda^2 \beta^2}{16} \right) x + \frac{\pi}{6} x^3 \right] \right\} \\
 & + B_1 \left\{ \frac{\lambda^2 \alpha^2}{2} \pi x - \lambda^4 \alpha^4 \left(\frac{5}{32} - \frac{3\gamma}{8} \right) \frac{\pi}{2} x + \frac{3}{8} \lambda^4 \alpha^4 \left[\frac{\pi}{4} \left(1 + \ln \frac{\lambda^2 \alpha^2}{16} \right) x + \frac{\pi}{6} x^3 \right] \right\} \\
 & + A_2 \left\{ -\frac{\lambda^4 \beta^2}{2} \frac{3\pi}{2} x + \frac{\lambda^4 \beta^2}{2} \pi x^3 \right\} \\
 & + B_2 \left\{ \frac{\lambda^4 \alpha^2}{2} \frac{3\pi}{2} x - \frac{\lambda^4 \alpha^2}{2} \pi x^3 \right\} + O(\lambda^6 \ln \lambda) = -\frac{m_0 \pi C^2}{i \lambda^2 R D} x
 \end{aligned} \tag{4.46}$$

Similarly:

$$\begin{aligned}
 & A_1 \left\{ -(4-\nu_0) \frac{\alpha^2 \lambda^2}{2} \pi x + \lambda^4 \beta^4 \left[\frac{5\nu_0-8}{32} + \frac{4-3\nu_0}{8} \gamma \right] \frac{\pi}{2} x + \lambda^4 \beta^4 \left(\frac{4-3\nu_0}{8} \right) \left[\frac{\pi}{4} \left(1 + \ln \frac{\lambda^2 \beta^2}{16} \right) x + \frac{\pi}{6} x^3 \right] \right\} \\
 & + B_1 \left\{ -(4-\nu_0) \frac{\beta^2 \lambda^2}{2} \pi x + \lambda^4 \alpha^4 \left[\frac{5\nu_0-8}{32} + \frac{4-3\nu_0}{8} \gamma \right] \frac{\pi}{2} x + \lambda^4 \alpha^4 \left(\frac{4-3\nu_0}{8} \right) \left[\frac{\pi}{4} \left(1 + \ln \frac{\lambda^2 \alpha^2}{16} \right) x + \frac{\pi}{6} x^3 \right] \right\} \\
 & + A_2 \left\{ -(4-\nu_0) \frac{\alpha^2 \lambda^4}{2} \left(\frac{3}{2} \pi x - \pi x^3 \right) \right\} \\
 & + B_2 \left\{ -(4-\nu_0) \frac{\beta^2 \lambda^4}{2} \left(\frac{3}{2} \pi x - \pi x^3 \right) \right\} + O(\lambda^6 \ln \lambda) = -m_0 \pi x
 \end{aligned} \tag{4.47}$$

Next we equate coefficients. In particular we first require the coefficients of the x^3 terms to vanish which gives

$$A_2 + B_2 = -\frac{\alpha^2}{8} (A_1 - B_1) \quad (4.48)$$

$$A_2 - B_2 = -\frac{4-3\nu_0}{4-\nu_0} \frac{\alpha^2}{24} (A_1 + B_1) \quad (4.49)$$

Then substituting 4.48 and 4.49 into 4.46 and 4.47 and solving for A_1 and B_1 we find

$$A_1 = \frac{\eta_0 c^2}{\lambda^4 R D} \left\{ 1 + \frac{\pi \lambda^2}{16} \frac{8-3\nu_0}{4-\nu_0} + \frac{\lambda^2 \alpha^2}{4-\nu_0} \left(\frac{8-7\nu_0}{32} + \frac{4-3\nu_0}{8} \gamma \right) + \frac{\lambda^2 \alpha^2}{16} \frac{4-3\nu_0}{4-\nu_0} \left(1 + \ln \frac{\lambda^2 \alpha^2}{16} \right) \right\} \quad (4.50)$$

$$+ \frac{m_0}{\lambda^2 \alpha^2 (4-\nu_0)} \left\{ 1 + \frac{\pi \lambda^2}{16} \frac{8-3\nu_0}{4-\nu_0} + \lambda^2 \alpha^2 \left(\frac{7}{32} + \frac{3\gamma}{8} \right) + \frac{3}{16} \lambda^2 \alpha^2 \left(1 + \ln \frac{\lambda^2 \alpha^2}{16} \right) \right\} + O(\lambda^2 \ln \lambda)$$

$$B_1 = \frac{\eta_0 c^2}{\lambda^4 R D} \left\{ 1 + \frac{\lambda^2 \pi}{16} \frac{8-3\nu_0}{4-\nu_0} + \frac{\lambda^2 \beta^2}{4-\nu_0} \left(\frac{8-7\nu_0}{32} + \frac{4-3\nu_0}{8} \gamma \right) + \frac{\lambda^2 \beta^2}{16} \frac{4-3\nu_0}{4-\nu_0} \left(1 + \ln \frac{\lambda^2 \beta^2}{16} \right) \right\} \quad (4.51)$$

$$+ \frac{m_0}{\lambda^2 \beta^2 (4-\nu_0)} \left\{ 1 + \frac{\lambda^2 \pi}{16} \frac{8-3\nu_0}{4-\nu_0} + \lambda^2 \beta^2 \left(\frac{7}{32} + \frac{3\gamma}{8} \right) + \frac{3}{16} \lambda^2 \beta^2 \left(1 + \ln \frac{\lambda^2 \beta^2}{16} \right) \right\} + O(\lambda^2 \ln \lambda)$$

We should point out that, if coefficients A_1 , B_1 of higher accuracy are desired, say up to order λ^{2n} , then it is necessary to solve an $n \times n$ algebraic system. In effect, this is a method of successive approximations for which the question of convergence will be investigated in Appendix II.

It thus appears that for $\lambda < \lambda^*$ the power series solutions of the form

$$u_1^{(N)}(\xi) = \sqrt{1-\xi^2} \sum_{n=0}^N A_{n+1} \lambda^{2n} (1-\xi^2)^n \quad (4.52)$$

$$u_2^{(N)}(\xi) = \sqrt{1-\xi^2} \sum_{n=0}^N B_{n+1} \lambda^{2n} (1-\xi^2)^n \quad (4.53)$$

in the limit as $N \rightarrow \infty$, will converge to the exact solutions $u_1(\xi)$ and $u_2(\xi)$ of the integral equations 4.38 and 4.39. However since most particular solutions will give us a non-uniform residual moment and normal membrane stress along the crack, it is only natural to ask how the solution changes. Suppose, for $|x| < 1$, we expand m_0 and n_0 in the form $\sum_n a_n x^{2n}$ (even powers because of the symmetry of the problem), then our previous method of solution will still be applicable. And as can easily be seen from equations 4.32 and 4.33, although the coefficients A_n, B_n in this case may change, the character of the solution will still remain the same. Finally, because we desire to focus our attention upon the singular stresses around the neighborhood of the crack point, we need only to compute coefficients A_1 and B_1 .

6. Determination of W and F

In view of equations 4.14, 4.15, 4.44, 4.45 and the relation

$$\int_0^\infty s^{-h} J_h(as) \cos xs ds = \begin{cases} \sqrt{\pi} (2a)^{-h} [\Gamma(h+\frac{1}{2})]^{-1} (\alpha^2-x^2)^{h-\frac{1}{2}}; & 0 < x < a \\ 0 & ; \alpha < x < \infty \end{cases} \quad ; \operatorname{Re} h > -\frac{1}{2} \quad (4.54)$$

which can be found on page 44 of [4] we have:

$$P_1(s) = \frac{s}{\sqrt{s^2-i\lambda^2}} \left\{ A_1 J_1(s) + 3\lambda^2 A_2 \frac{J_2(s)}{s} + O(\lambda^4) \right\} \quad (4.55)$$

and similarly

$$P_2(s) = \frac{s}{\sqrt{s^2 + i\lambda^2}} \left\{ B_1 J_1(s) + 3\lambda^2 B_2 \frac{J_2(s)}{s} + O(\lambda^4) \right\} \quad (4.56)$$

where A_1 and B_1 are given by 4.50 and 4.51 respectively. And finally substituting 4.55 and 4.56 into 4.5 and 4.10 we find

$$P_3(s) = - (A_1 + B_1) J_1(s) - 3\lambda^2 (A_2 + B_2) \frac{J_2(s)}{s} - \frac{i\lambda^2}{\nu_0 s^2} (A_1 - B_1) J_1(s) + O(\lambda^4) \quad (4.57)$$

and

$$P_4(s) = - (A_1 - B_1) J_1(s) - 3\lambda^2 (A_2 - B_2) \frac{J_2(s)}{s} + O(\lambda^4) \quad (4.58)$$

Therefore, a substitution of the above relations into 4.1 and 4.2 will determine the bending deflection W and membrane stress function F .

7. Determination of the Singular Stresses

In view of equations 4.1, 4.2, 4.55, 4.56, the bending and extensional stresses defined by 1.9-1.14 can be expressed in integral forms which may then be evaluated using the relations 14-17 of Appendix I. Without going into the details we list below the results.

Bending stresses*: On the surface $Z = + \frac{h}{2}$

$$\sigma_{xb} = - \frac{ER}{2(1+\nu)c^2} \frac{\tilde{P}_{10}}{\sqrt{E}} \left(\frac{3}{4} \cos \frac{\theta}{2} + \frac{1}{4} \cos \frac{5\theta}{2} \right) + O(\epsilon^0) \quad (4.59)$$

$$\sigma_{yb} = \frac{ER}{2(1-\nu^2)c^2} \frac{\tilde{P}_{10}}{\sqrt{E}} \left(\frac{11+5\nu}{4} \cos \frac{\theta}{2} + \frac{1-\nu}{4} \cos \frac{5\theta}{2} \right) + O(\epsilon^0) \quad (4.60)$$

* Note because of the Kirchhoff boundary conditions, the bending shear stress does not vanish in the free edge. For the flat sheet this problem was discussed by Knowles and Wang [7].

$$\tilde{\tau}_{xy_b} = \bar{\sigma} \frac{Gh}{(1-\nu)c^2} \frac{\tilde{P}_{10}}{\sqrt{E}} \left(\frac{1+\nu}{4} \sin \frac{\theta}{2} + \frac{1-\nu}{4} \sin \frac{5\theta}{2} \right) + O(\epsilon^0) \quad (4.61)$$

where the ~~tilde~~ signs refer to $\nu > 0$ and $\nu < 0$ respectively and

$$\begin{aligned} \tilde{P}_{10} \equiv \alpha^2 \lambda^2 \frac{A_1 - B_1}{2\sqrt{2}} = & - \frac{\eta_0 \lambda^2}{\sqrt{2ERD}(4-\nu_0)} \left\{ \frac{8-7\nu_0}{32} + \frac{4-3\nu_0}{8} \nu + \frac{4-3\nu_0}{16} (1 + \ln \frac{\lambda^2}{16}) \right\} \\ & + \frac{\eta_0}{\sqrt{2}(4-\nu_0)} \left\{ 1 + \frac{\pi \lambda^2}{32} \frac{4-3\nu_0}{4-\nu_0} \right\} + O(\lambda^4 \ln \lambda) \end{aligned} \quad (4.62)$$

Similarly

Extensional stresses:

$$\tilde{\sigma}_{x_c} = \frac{\tilde{P}_{20}}{Rc^4 \sqrt{E}} \left(\frac{3}{4} \cos \frac{\theta}{2} + \frac{1}{4} \cos \frac{5\theta}{2} \right) + O(\epsilon^0) \quad (4.63)$$

$$\tilde{\sigma}_{y_c} = \frac{\tilde{P}_{20}}{Rc^4 \sqrt{E}} \left(\frac{5}{4} \cos \frac{\theta}{2} - \frac{1}{4} \cos \frac{5\theta}{2} \right) + O(\epsilon^0) \quad (4.64)$$

$$\tilde{\tau}_{xy_c} = \bar{\sigma} \frac{\tilde{P}_{20}}{Rc^4 \sqrt{E}} \left(\frac{1}{4} \sin \frac{\theta}{2} - \frac{1}{4} \sin \frac{5\theta}{2} \right) + O(\epsilon^0) \quad (4.65)$$

where

$$\begin{aligned} \tilde{P}_{20} \equiv \frac{\lambda^4 RD}{2\sqrt{2}} (A_1 + B_1) \\ = \frac{\eta_0 c^2}{\sqrt{2}} \left\{ 1 + \frac{3\pi}{32} \lambda^2 \right\} + \frac{\eta_0 \lambda^2 \sqrt{ERD} c^2}{\sqrt{2}(4-\nu_0)} \left\{ \frac{13}{32} + \frac{3\nu}{8} + \frac{3}{16} \ln \frac{\lambda^2}{16} \right\} \\ + O(\lambda^4 \ln \lambda). \end{aligned} \quad (4.66)$$

It is apparent from the above equations that there exists an interaction between bending and stretching, except that in the limit as $\lambda \rightarrow 0$ the stresses of a flat sheet are recovered and coincide with those obtained

previously for bending [8] and extension [9]. Thus the stresses in a shell are expressed in terms of the stresses in a flat sheet.

8. Combined Stresses

In general, the combined stresses will depend upon the contributions of the particular solutions reflecting the magnitude and distribution of the applied normal pressure. On the other hand the singular part of the solution, that is the terms producing infinite elastic stresses at the crack tip, will depend only upon the local stresses existing along the locus of the crack before it is cut, which of course are precisely the stresses which must be removed or cancelled by the particular solutions described above in order to obtain the stress free edges as required physically. Hence the distribution of $q(x,y)$ does not — to the first order — affect the local character of the stresses at the crack point.

CHAPTER V

SOLUTION OF THE ANTISYMMETRIC PART

1. Integral Representations and the Stresses

It can be shown* that the kernels are given in terms of

$$\int_0^{\infty} \frac{1}{s} e^{-\sqrt{s^2 - \lambda^2 \alpha^2} |y|} \sin \zeta s ds$$

which we cannot evaluate in a closed form. Therefore, we will restrict ourselves to the special case where $v_0 = 0$ and $t_0 \neq 0$ but a constant. In view of the above, we can assume the following integral representations of the solutions

$$W(x, y^{\pm}) = \mp \int_0^{\infty} \left\{ Q_5 e^{-\sqrt{s^2 - i\lambda^2} |y|} + Q_6 e^{-\sqrt{s^2 + i\lambda^2} |y|} + Q_7 e^{-s|y|} \right\} \sin xs ds \quad (5.1)$$

$$F(x, y^{\pm}) = \mp \frac{i\lambda^2 R D}{c^2} \int_0^{\infty} \left\{ Q_5 e^{-\sqrt{s^2 - i\lambda^2} |y|} - Q_6 e^{-\sqrt{s^2 + i\lambda^2} |y|} + Q_8 e^{-s|y|} \right\} \sin xs ds \quad (5.2)$$

where again the \mp signs refer to $y > 0$ and $y < 0$ respectively. Without going into details (see Appendix III) we list below the results for $Z = \frac{h}{2}$

$$\sigma_{x_b} = \pm \frac{ER}{2(1-\nu^2)} \frac{\alpha^2 \lambda^2 \tilde{P}_{30}}{2\sqrt{2}E c^2} \left(\frac{9+7\nu}{4} \sin \frac{\theta}{2} - \frac{\nu_0}{4} \sin \frac{5\theta}{2} \right) + O(\epsilon^0) \quad (5.3)$$

$$\sigma_{y_b} = \mp \frac{ER\nu_0}{2(1-\nu^2)} \frac{\alpha^2 \lambda^2 \tilde{P}_{30}}{2\sqrt{2}E c^2} \left(\frac{1}{4} \sin \frac{\theta}{2} - \frac{1}{4} \sin \frac{5\theta}{2} \right) + O(\epsilon^0) \quad (5.4)$$

$$\tau_{xy_b} = - \frac{GR}{2\nu_0} \frac{\alpha^2 \lambda^2 \tilde{P}_{30}}{\sqrt{2}E c^2} \left(\frac{8-3\nu_0}{4} \cos \frac{\theta}{2} - \frac{\nu_0}{4} \cos \frac{5\theta}{2} \right) + O(\epsilon^0) \quad (5.5)$$

$$\sigma_{x_e} = \mp \frac{i\lambda^4 R D \alpha^2}{2\sqrt{2}E R c^4} \tilde{P}_{40} \left(\frac{7}{4} \sin \frac{\theta}{2} + \frac{1}{4} \sin \frac{5\theta}{2} \right) + O(\epsilon^0) \quad (5.6)$$

* For more details see Appendix III.

$$\tilde{G}_{ye} = \mp \frac{i\lambda^4 RD \alpha^2}{2\sqrt{2}\epsilon^2 RC^4} \tilde{P}_{40} \left(\frac{1}{4} \sin \frac{\theta}{2} - \frac{1}{4} \sin \frac{5\theta}{2} \right) + O(\epsilon^0) \quad (5.7)$$

$$\tilde{T}_{xye} = \frac{i\lambda^4 RD \alpha^2}{2\sqrt{2}\epsilon^2 RC^4} \tilde{P}_{40} \left(\frac{3}{4} \cos \frac{\theta}{2} + \frac{1}{4} \cos \frac{5\theta}{2} \right) + O(\epsilon^0) \quad (5.8)$$

where

$$\tilde{P}_{40} \equiv \frac{2t_0 c^2}{\lambda^4 RD} \left\{ 1 + \frac{\pi\lambda^2}{32} + O(\lambda^2 \ln \lambda) \right\} \quad (5.9)$$

$$\tilde{P}_{30} \equiv \frac{c^2 \lambda^2 \alpha^2 t_0}{\lambda^4 RD} \left\{ \frac{\nu_0 - 8 + 4(4 + \nu_0)\delta}{16\nu_0} + \frac{4 + \nu_0}{8\nu_0} \ln \frac{\lambda^2}{16} + O(\lambda^2 \ln \lambda) \right\} \quad (5.10)$$

which, for the case $\lambda = 0$, also limit check the results in refs. [8] and [9].

CHAPTER VI

A PARTICULAR SOLUTION

As an illustration of how the local solution may be combined in a particular case, consider a clamped segment of a shallow spherical shell of base radius \bar{R}_0 and containing at the apex a finite radial crack of length $2c$ in the direction of the X-axis (see fig. 2). The shell is subjected to a uniform internal pressure q_0 with radial extension $N_r = \frac{1}{2} q_0 R$, and because it is clamped we require that the displacement and slope vanish at $\bar{R} = \bar{R}_0$. For this problem, Reissner [10] gives the solution of the coupled-extension-bending equations for the uncracked shell as:

$$W_p(\tau) = c_1 \text{ber}(\lambda\tau) + c_2 \text{bei}(\lambda\tau) + c_3 \quad (6.1)$$

$$F_p(\tau) = \frac{Eh^2}{\sqrt{12(1-\nu^2)}} \left\{ c_1 \text{bei}(\lambda\tau) - c_2 \text{ber}(\lambda\tau) \right\} - \frac{1}{4} q_0 R \tau^2 \quad (6.2)$$

where

$$c_1 = \frac{c^2 q_0 R \sqrt{12(1-\nu^2)} \tau_0}{Eh^2 \lambda} \frac{\text{bei}'(\lambda\tau_0)}{[\text{bei}'(\lambda\tau_0)]^2 + [\text{ber}'(\lambda\tau_0)]^2}$$

$$c_2 = -c_1 \left\{ \frac{\text{ber}'(\lambda\tau_0)}{\text{bei}'(\lambda\tau_0)} \right\}$$

$$c_3 = -c_1 \left\{ \frac{\text{ber}(\lambda\tau_0) \text{bei}'(\lambda\tau_0) - \text{bei}(\lambda\tau_0) \text{ber}'(\lambda\tau_0)}{\text{bei}'(\lambda\tau_0)} \right\}$$

Along any radial ray, and in particular along $\theta = 0, \pi$, the bending and extensional shear vanish by symmetry, and the circumferential bending and stretching stresses are

$$M_{\theta\theta}^{(P)}(\tau) = \frac{D\lambda^2}{c^2} \left\{ c_1 \left[\nu \operatorname{bei}(\lambda\tau) - (1-\nu) \frac{\operatorname{ber}'(\lambda\tau)}{\lambda\tau} \right] - c_2 \left[\nu \operatorname{ber}(\lambda\tau) + (1-\nu) \frac{\operatorname{bei}'(\lambda\tau)}{\lambda\tau} \right] \right\} \quad (6.3)$$

$$N_{\theta\theta}^{(P)}(\tau) = \frac{E\lambda^2(\lambda^2/c^2)}{\sqrt{12(1-\nu^2)}} \left\{ c_1 \operatorname{bei}''(\lambda\tau) - c_2 \operatorname{ber}''(\lambda\tau) \right\} - \frac{1}{2} q_0 R \quad (6.4)$$

$$N_{\tau\theta}(\tau) = 0 \quad (6.5)$$

$$V_{\tau\theta}(\tau) = 0 \quad (6.6)$$

Therefore, the homogeneous solution must negate these values from the particular solution. But since in Chapter IV we already have obtained a solution for uniform loadings along the crack, * namely m_0 and n_0 , therefore we will make use of these results in order to obtain an estimate of the stresses in the vicinity of the crack. As an engineering approximation, by considering an upper and lower bound on m_0 and n_0 , we may estimate an upper and lower bound for the stresses in the neighborhood of the crack point. On the other hand, if we are interested in the stresses away from the crack, say 3 times the crack length, then by Saint Venant's principle we need to take only the average values. Thus we define

$$\frac{D m_0^{(L)}}{c^2} = \min_{|x| < 1, \theta = 0} M_{\theta\theta}^{(P)} \leq \frac{D m_{+max}}{c^2} \leq \max_{|x| < 1, \theta = 0} M_{\theta\theta}^{(P)} = D \frac{m_0^{(U)}}{c^2}$$

* For non-uniform see remark in sect. 5, Chapter IV.

and similarly

$$\frac{\eta_o^{(q)}}{c^2} = \min_{|x| < 1, \theta = 0} N_{\theta\theta}^{(P)} \leq \frac{\eta_{+ave}}{c^2} \leq \max_{|x| < 1, \theta = 0} N_{\theta\theta}^{(P)} = \frac{\eta_o^{(u)}}{c^2}$$

Next, let us consider a spherical shell with the following geometrical dimensions:

$$\bar{R}_o = 4.25 \text{ in.}$$

$$R = 20 \text{ in.}$$

$$h = 0.009 \text{ in.}$$

$$\nu = 1/3$$

$$2c = 0.46 \text{ in.}$$

$$E = 16 \times 10^6 \text{ psi}$$

from which we can calculate the parameters

$$\lambda = 0.98$$

$$r_o = 18.50$$

The following table shows the variation of the residual moment $M_{\theta\theta}^{(P)}$ and membrane force $N_{\theta\theta}^{(P)}$ along the crack.

X	$\lambda x = \lambda \frac{X}{c}$	$N_{\theta\theta}^{(P)}$	$M_{\theta\theta}^{(P)}$
0	0	-0.50 $q_o R$	$0.89 \times 10^{-4} q_o Rh$
0.074	0.30	-0.50 $q_o R$	$0.87 \times 10^{-4} q_o Rh$
0.117	0.50	-0.50 $q_o R$	$0.92 \times 10^{-4} q_o Rh$
0.164	0.70	-0.50 $q_o R$	$0.94 \times 10^{-4} q_o Rh$
0.235	1.00	-0.50 $q_o R$	$0.97 \times 10^{-4} q_o Rh$
		diff. 0%	diff. 9%

It is clear from the table above that $M_{\theta\theta}^{(P)}$ and $N_{\theta\theta}^{(P)}$ are almost uniform along the crack. Therefore we may choose

$$\frac{\eta_0^{(u)}}{c^2} = 0.50 f_0 R$$

$$\frac{Dm_0^{(u)}}{c^2} = -0.97 \times 10^{-4} f_0 R h$$

Returning now to the stresses along the crack prolongation, for example the normal stress $\sigma_{y_{total}}(X, 0)$, one finds using 4.60 and 4.64 that:

$$\sigma_{y_{total}}(X, 0) \Big|_{\nu=\frac{1}{3}} \approx \frac{\bar{\sigma}_b}{\sqrt{2(X-1)/c}} \left\{ 1 + (0.16 + 0.03 \ln \frac{\lambda^2}{16}) \lambda^2 \right\}$$

$$+ \frac{\bar{\sigma}_e}{\sqrt{2(X-1)/c}} \left\{ 1 - (0.38 + 0.23 \ln \frac{\lambda^2}{16}) \lambda^2 \right\}$$
(6.8)

which for $\lambda = 0.98$ reduces to:

$$\sigma_{y_{total}}(X, 0) \approx \frac{\bar{\sigma}_b}{\sqrt{2(X-1)/c}} \{ 1.07 \} + \frac{\bar{\sigma}_e}{\sqrt{2(X-1)/c}} \{ 1.27 \}$$
(6.9)

where

$$\bar{\sigma}_b = \frac{6D}{h^2} \frac{m_0}{c^2} = \text{"applied bending"}$$

$$\bar{\sigma}_e = \frac{m_0}{c^2 h} = \text{"applied stretching"}$$

And for our particular example, we can associate

$$\bar{\sigma}_b^{(u)} \approx -0.58 \times 10^{-3} \frac{f_0 R}{h} \approx -0.001 \frac{f_0 R}{h}$$
(6.10)

$$\bar{\sigma}_e^{(u)} \approx 0.50 \frac{f_0 R}{h}$$
(6.11)

From equation 6.9 we see that the initial curvature will increase the applied bending stress by approximately 7% and the applied stretching

stress by 27%. One deduces therefore that the critical crack length of a shell decreases with an increase of λ or a decrease of radius of curvature. (See next section.) In this particular case it is found that the direct bending stresses are negligible compared to the extensional ones and the combined stress is

$$\sigma_{y_{total}}(\bar{x}, 0) \Big|_{\nu=\frac{1}{3}} \approx \frac{0.64}{\sqrt{2(\bar{x}-1)}} \frac{f_0 R}{h} = \frac{0.64 \sqrt{c}}{\sqrt{2(\bar{x}-1)}} \frac{f_0 R}{h} \quad (6.12)$$

and similarly

$$\sigma_{x_{total}}(\bar{x}, 0) \Big|_{\nu=\frac{1}{3}} \approx \frac{0.64 \sqrt{c}}{\sqrt{2(\bar{x}-1)}} \frac{f_0 R}{h} \quad (6.13)$$

where, based on the Kirchhoff theory, the two-dimensional "hydrostatic tension" nature of the σ_x and σ_y stresses predicted for flat plates is preserved. Finally, the corresponding strains are

$$\epsilon_y(\bar{x}, 0) \approx 0.30 \sqrt{\frac{c}{\bar{x}-1}} \frac{f_0 R}{Eh} \quad (6.14)$$

$$\epsilon_x(\bar{x}, 0) \approx 0.30 \sqrt{\frac{c}{\bar{x}-1}} \frac{f_0 R}{Eh} \quad (6.15)$$

CHAPTER VII

GRIFFITH'S THEORY OF FRACTURE FOR CURVED SHEETS

As is well known in fracture mechanics, the prediction of failure in the presence of sharp discontinuities is a very complicated problem. Some work has been done on flat sheets, based on the brittle fracture theory of A. A. Griffith [11]. His hypothesis is that the total energy of a cracked system subjected to loading remains constant as the crack extends an infinitesimal distance. It should of course be recognized that this is a necessary condition for failure but not sufficient.

Griffith applied his criterion to an infinite, isotropic plate containing a flat, sharp-ended crack of length $2c$. We shall now proceed to obtain a similar, but approximate, criterion for initially curved sheets based upon only the singular terms of the stresses.

The basic concept for crack instability is

$$\frac{\partial U_{\text{system}}}{\partial c} = 0 \quad (7.1)$$

where the system energy is defined by

$$U_{\text{system}} = U_{\text{loading}} + U_{\text{strain}} + U_{\text{surface}} \quad (7.2)$$

The applied stresses are held constant so that

$$U_{\text{loading}} = U_0 - h \int_P (\sigma_{\xi\xi} u_{\eta} + \tau_{\xi\eta} u_{\eta}) dP \quad (7.3)$$

where U_0 is a reference constant energy, and the integration is over that portion of the outer perimeter where forces act to cause displacements. The strain energy is

$$U_{\text{strain}} = \frac{1}{2} \int_{\text{vol}} (\sigma_{\xi} \epsilon_{\xi} + \tau_{\xi\eta} \gamma_{\xi\eta} + \sigma_{\eta} \epsilon_{\eta}) d\text{vol.} \quad (7.4)$$

$$U_{\text{surface}} = \gamma (2s + ph + 4ch) \quad (7.5)$$

It may be shown that the surface area S of the shell faces and the outer perimeter P of the shell are independent of the crack length.

Therefore 7.2 may be written as

$$U_{\text{system}} = U_0' + 4\gamma^* hc - h \int_P (\sigma_{\xi} u_{\xi} + u_{\eta} \tau_{\xi\eta}) dP + \frac{1}{2} \int_{\text{vol}} (\sigma_{\xi} \epsilon_{\xi} + \tau_{\xi\eta} \gamma_{\xi\eta} + \sigma_{\eta} \epsilon_{\eta}) d\text{vol.}$$

or

(7.6)

$$U_{\text{system}} = U_0' + 4\gamma^* c -$$

$$- \lim_{\epsilon \rightarrow 0} \frac{c}{8G} \int_{Z_1}^{Z_2} \int_{\epsilon}^{A^*} \int_{-n}^n \left\{ \frac{1-\nu}{1+\nu} (\sigma_c + \sigma_b)^2 + (\sigma_c - \sigma_b)^2 + (2\tau_{rb})^2 \right\} R^2 dR^2 d\theta dz$$

where $U_0' = U_0 + \gamma^* (2A + Ph)$, $Z_1 = Z_0 - \frac{h^*}{2}$, $Z_2 = Z_0 + \frac{h^*}{2}$ and A^* a radius to be determined (see fig. 3). In the above we have defined

$$\frac{h^*}{2} = R \left[\sqrt{1 - \left(\frac{R - R/2}{R} \right)^2} \frac{\bar{R}^2}{R^2} - \frac{R - R/2}{R} \sqrt{1 - \frac{\bar{R}^2}{R^2}} \right]$$

$$Z_0 = \sqrt{R^2 - \bar{R}^2} - (R - \delta)$$

with δ the height of the shell segment.

Integration of 7.6 with respect to θ gives:

$$U_{\text{system}} = U_0' + 4\gamma c h - \lim_{\epsilon \rightarrow 0} \frac{c\pi}{8G} \int_{Z_1}^{Z_2} \int_{\epsilon}^{A^*} I_1 dR^* dZ \quad (7.7)$$

where

$$I_1 = \frac{1-\nu}{1+\nu} \left[(k_0 + k_2)^2 + (k_1 + k_3)^2 \right] + \left[(k_0 - k_2)^2 + (k_1 - k_3)^2 \right] \quad (7.8)$$

with

$$k_0 + k_2 = \frac{EZ}{c^2} \frac{2 \tilde{P}_{10}}{(1-\nu)} + \frac{2}{R} \frac{\tilde{P}_{20}}{c^4} \quad (7.9)$$

$$k_0 - k_2 = -\frac{EZ}{2c^2} \frac{7+\nu}{1-\nu^2} \tilde{P}_{10} - \frac{1}{2R} \frac{\tilde{P}_{20}}{c^4} \quad (7.10)$$

$$k_1 + k_3 = 0 \quad (7.11)$$

$$k_1 - k_3 = -\frac{EZ}{(1+\nu)} \frac{\tilde{P}_{10}}{2c^2} + \frac{1}{2R} \frac{\tilde{P}_{20}}{c^4} \quad (7.12)$$

And since we are restricting ourselves to the singular stresses, it is only fair to derive a Griffith criterion applicable in the immediate neighborhood of the crack tip, where because locally the shell is almost flat, we can replace without much error the limits of integration Z_1 and Z_2 by $-\frac{h}{2}$ and $\frac{h}{2}$. Thus 7.7 may be approximated by

$$U_{\text{system}} = U_0' + 4\gamma^* c h - \lim_{\epsilon \rightarrow 0} \frac{c\pi}{8G} \int_{-\frac{h}{2}}^{\frac{h}{2}} \int_{\epsilon}^{A^*} I_1 dR^* dZ \quad (7.13)$$

and after integration

$$U_{\text{system}} = U_0' + 4\gamma^* c h$$

$$\begin{aligned} & -\frac{c\pi}{8G} \left\{ \frac{1-\nu}{1+\nu} \left(\frac{2E\tilde{P}_{10}}{c^2(1-\nu)} \right)^2 \frac{2}{3} \left(\frac{R}{2} \right)^3 + \frac{1-\nu}{1+\nu} \left(\frac{2}{R} \frac{\tilde{P}_{20}}{c^4} \right)^2 h \right. \\ & \left. + \frac{\nu^2+6\nu+25}{3(1-\nu^2)^2} \frac{E^2\tilde{P}_{10}^2}{c^4} \left(\frac{R}{2} \right)^3 + \frac{1}{2} \frac{\tilde{P}_{20}^2}{R^2 c^8} h \right\} A^* \end{aligned} \quad (7.14)$$

which in the limit, as $R \rightarrow \infty$ and $\bar{\sigma}_b \rightarrow 0$, in equal biaxial tension $\bar{\sigma}_e$ along the periphery of a flat sheet, must equal to (see ref. [12])

$$U_{\text{system}} = U_0' + 4\gamma^* c h - \frac{5h}{4G} (R-1) \bar{\sigma}_e^2 - \frac{\pi c^2 h}{8G} (3-R) \bar{\sigma}_e^2 \quad (7.15)$$

Thus we have determined the value for A^* , namely

$$A^* = \frac{16\nu c}{9-7\nu} + \frac{16(1-\nu)}{9-7\nu} \frac{5}{\pi c} \quad (7.16)$$

Substituting in 7.14 for A^* and applying the basic condition 7.1, the fracture criterion is seen to be:

$$\begin{aligned} & 4\gamma^* h - \frac{\pi c}{4G} \left\{ \frac{33+6\nu-7\nu^2}{(1-\nu^2)^2} \frac{E^2 \tilde{P}_{10}^2 h^3}{c^4} + \right. \\ & \left. + \frac{9-7\nu}{2(1+\nu)} \frac{\tilde{P}_{20}^2}{h c^8} \right\} \frac{16\nu}{9-7\nu} = 0 \end{aligned} \quad (7.17)$$

where

$$\tilde{P}_{10} = -\frac{c^4 h \bar{\sigma}_e}{\sqrt{2} R D (4-\nu_0)} \left\{ \frac{16-13\nu_0}{32} + \frac{4-3\nu_0}{8} \left(\gamma + \ln \frac{\lambda}{4} \right) \right\} \quad (7.18)$$

$$+ \frac{h^2 c^2 \bar{\sigma}_b}{6\sqrt{2} (4-\nu_0) D} \left\{ 1 + \frac{\pi}{32} \frac{4-3\nu_0}{4-\nu_0} \lambda^2 \right\} + O(\lambda^4 \ln \lambda)$$

and

$$\bar{P}_{20} = \frac{c^4 R \bar{\sigma}_e}{\sqrt{2}} \left\{ 1 + \frac{3\pi}{32} \lambda^2 \right\} + \frac{R^2 c^2 \lambda^4 R \bar{\sigma}_b}{6\sqrt{2} (4-\nu_0)} \left\{ \frac{13}{32} + \frac{3}{8} \left(\gamma + 4 \ln \frac{\lambda}{4} \right) \right\} + O(\lambda^4 \ln \lambda) \quad (7.19)$$

Finally introducing 7.18 and 7.19 into 7.17 we arrive after some re-arrangement at:

$$\begin{aligned} & \frac{(33+6\nu-7\nu^2)4\nu}{3(9-7\nu)(4-\nu_0)^2} \left(1 + \frac{\pi}{16} \frac{4-3\nu_0}{4-\nu_0} \lambda^2 \right) \bar{\sigma}_b^2 + \frac{4\nu}{1+\nu} \left(1 + \frac{3\pi}{16} \lambda^2 \right) \bar{\sigma}_e^2 \\ & + \left[-\frac{8}{\sqrt{3}} \frac{(33+6\nu-7\nu^2)\nu}{\sqrt{1-\nu^2}(9-7\nu)(4-\nu_0)^2} \left(\frac{16-3\nu_0}{32} + \frac{4-3\nu_0}{8} \gamma + \frac{4-3\nu_0}{8} \ln \frac{\lambda}{4} \right) \right. \\ & \left. + \frac{8\nu}{\sqrt{3}} \sqrt{\frac{1-\nu}{1+\nu}} \frac{1}{(4-\nu_0)} \left(\frac{13}{32} + \frac{3}{8} \gamma + \frac{3}{8} \ln \frac{\lambda}{4} \right) \right] \lambda^2 \bar{\sigma}_e \bar{\sigma}_b = \frac{16G\gamma^*}{\pi c} \end{aligned} \quad (7.20)$$

which, for the case of a flat sheet, i.e. $\lambda = 0$, reduces to the following simple form:

$$\left(\frac{33+6\nu-7\nu^2}{3(4-\nu_0)^2(9-7\nu)} \right) 4\nu \bar{\sigma}_b^2 + \frac{4\nu}{1+\nu} \bar{\sigma}_e^2 = \frac{16G\gamma^*}{\pi c_p} \equiv (\sigma_p^*)^2 \quad (7.21)$$

For $\nu = \frac{1}{3}$ equation 7.20 becomes

$$\begin{aligned} & \overset{0.21}{0.29} (1 + 0.12 \lambda^2) \bar{\sigma}_b^2 + (1 + 0.59 \lambda^2) \bar{\sigma}_e^2 \\ & - \underbrace{(0.42 + 0.14 \ln \frac{\lambda}{4})}_{(0.24 + 0.07 \ln \frac{\lambda}{4})} \lambda^2 \bar{\sigma}_e \bar{\sigma}_b = \frac{16G\gamma^*}{\pi c} \equiv (\sigma_s^*)^2 \end{aligned} \quad (7.22)$$

which clearly represents a family of ellipses. In view of 7.22 we can obtain a relation between the critical crack length in a shell and the critical crack length in a plate, i.e. for $\nu = \frac{1}{3}$

$$(l_{cr})_{shell} = \frac{\left[\overset{0.21}{0.29} \bar{\sigma}_b^2 + \bar{\sigma}_e^2 \right]_{plate} (l_{cr})_{plate}}{\left[\overset{0.21}{0.29} (1 + 0.12 \lambda^2) \bar{\sigma}_b^2 + (1 + 0.59 \lambda^2) \bar{\sigma}_e^2 - \underbrace{(0.42 + 0.14 \ln \frac{\lambda}{4})}_{(0.24 + 0.07 \ln \frac{\lambda}{4})} \lambda^2 \bar{\sigma}_e \bar{\sigma}_b \right]_{shell}} \quad (7.23)$$

for example if $\lambda = 1$ and $(\bar{\sigma}_b)_P = (\bar{\sigma}_b)_S = (\bar{\sigma}_e)_S = (\bar{\sigma}_e)_P$, then 7.23 reduces to:

$$(l_{cr})_{shell} \approx 0.76 (l_{cr})_{plate} \quad \checkmark \quad (7.24)$$

This clearly shows that the critical crack length for a spherical shell is less than that of a flat sheet, and as is seen by 7.23 the ratio depends upon the curvature. This agrees with the statement following equations 6.10 and 6.11.

For the special case where $(\bar{\sigma}_b)_P = (\bar{\sigma}_b)_S = (\bar{\sigma}_e)_S = (\bar{\sigma}_e)_P$ we obtain the following expression

$$\left(\frac{l_s}{l_P}\right)_{cr} = \frac{1}{1 + \frac{0.16 - 0.11 \ln \frac{\lambda}{4}}{0.31 - 0.06 \ln \frac{\lambda}{4}} \lambda^2} \quad (7.25)$$

This ratio is less than 1 for all $\lambda < 7$. We conjecture that for $\lambda > 7$ the same character will possibly be preserved, but more terms, say up to λ^4 , would be required to verify this point. As we have indicated, however, (see sect. 4, Chapter 4) for most practical cases λ is less than 2 hence 7.25 gives a good approximation. A plot of equation 7.25 is given in fig. 4.

Returning to equation 7.22 we note that it can also be written in the form

$$\begin{aligned} (1 + 0.59 \lambda^2) \left(\frac{\bar{\sigma}_e}{\bar{\sigma}_s^*}\right)^2 - \frac{(0.24 + 0.07 \ln \frac{\lambda}{4})}{(0.12 + 0.14 \ln \frac{\lambda}{4})} \lambda^2 \left(\frac{\bar{\sigma}_e}{\bar{\sigma}_s^*}\right) \cdot \left(\frac{\bar{\sigma}_b}{\bar{\sigma}_s^*}\right) + \\ + \frac{0.21}{0.29} (1 + 0.12 \lambda^2) \left(\frac{\bar{\sigma}_b}{\bar{\sigma}_s^*}\right)^2 = 1 \end{aligned} \quad (7.26)$$

This obviously represents a family of ellipses, which are plotted for different values of the parameter λ , see fig. 5. For λ greater than 1.5 we will need higher orders of λ for the determination of the ellipses; therefore for $\lambda = 10, 20$ we show just the intercepts.* It is also clear from fig. 5 that the applied safe load in a cracked spherical shell decreases with a decrease in radius of curvature. For example, if along the crack there is a residual load of equal bending and stretching a flat sheet can carry, before failure occurs, up to a load of $0.88 \left(\frac{\tilde{\sigma}_e}{\sigma^*} \right)$ while a spherical shell characterized with the parameter $\lambda = 1$ can carry only up to $0.76 \left(\frac{\tilde{\sigma}_e}{\sigma^*} \right)$, i.e. approximately 14% less load than a flat sheet.

* Curve for $\lambda = 2$ follows the anticipated trend.

CHAPTER VIII

EXPERIMENTAL VERIFICATION

8.1 Description of Experiment

To compare theoretical and actual behavior of an initially curved specimen, a preliminary experiment was conducted. We have considered a clamped segment of a shallow spherical shell, containing at the apex a radial cut of length 0.46 in. The shell was subjected to a uniform internal pressure q_0 , and the strain ϵ_y at three different positions along the direction of crack prolongation was recorded as a function of q_0 . The design of the experiment did not permit a determination of critical crack length, furthermore the copper material is too ductile for brittle fracture theory to apply.

8.2 Preparations

The shallow shell segment was constructed by the method of "copper electroforming."* Its characteristics were $h = 0.009$ in., $R = 20$ in., $\delta = 0.4$ in., $\bar{R}_0 = 4.25$ in., $\nu = \frac{1}{3}$, $E = 16 \times 10^6$ lbs/in². A hole of 0.014 in. diameter was drilled at the apex of the shell segment, and a crack was sawed with a jeweler's saw of 0.007 in. thickness. Finally, the ends of the crack were smoothed by the "diamond thread method,"** (diameter of diamond thread less than 0.005 in.). In the process of drilling and of sawing, a wax backing was used in order to avoid damaging of the shell. Next, along the crack prolongation, three strain gages were attached on the shell

* See ref. [13].

** A cotton thread impregnated with 6 micron diamond paste.

to measure the strains in the Y direction (see figs. 6, 7). The shell was cemented between two circular rings, with $\bar{R}_0 = 4$ in. as the inside radius (see fig. 8). Next the crack was sealed internally with two layers of acetate fibre tape. The first layer was a square of 2 x 2 inches, and the second layer was a rectangular one of 2 x $\frac{1}{2}$ inches. The following table gives the gage factors and positions of the gages from the crack tip.

<u>Gage no.</u>	<u>G.F. = Gage Factor</u>	<u>X - 1</u>	$\sqrt{\frac{C}{X-1}}$
1	2.10	0.07	1.81
2	2.09	0.29	0.89
3	2.09	0.48	0.69

In fig. 9 we have plotted voltage vs. gage pressure, and because the curves for small pressures were not quite straight lines, a second run was conducted a few hours later. It gave better results (fig. 10). The change between first and second runs is attributed to warming up of the resistance gages in the electronic equipment and "setting" of the strain gages. Even for the second run, the curves are slightly curved at the origin. It is possible that the tape carries a small part of the load. In any case, we consider the slope of the curve which is given by

$$C = \text{slope} = \frac{\Delta E \text{ voltage}}{A.F. \times \Delta q_0} \quad (8.1)$$

where A.F. = amplifier factor = 5

In view of this, we can compute the strains from

$$E_{y_{exp}} = \frac{4}{P.S.V.} \frac{C q_0}{G, F} \quad (8.2)$$

where P.S.V. = Power supply voltage = 6 volts (measured).

The theoretical strains were calculated from equation 6.14 and the comparison with experimentally determined values follows.

Gage No.	Theoretical ϵ_y	C	Exp. ϵ_y	C_1	Exp. ϵ_y
1	$0.75 \times 10^{-4} q_0$	3.03×10^{-4}	$0.96 \times 10^{-4} q_0$	2.42×10^{-4}	$0.77 \times 10^{-4} q_0$
2	$0.37 \times 10^{-4} q_0$	1.70×10^{-4}	$0.54 \times 10^{-4} q_0$	1.37×10^{-4}	$0.44 \times 10^{-4} q_0$
3	$0.29 \times 10^{-4} q_0$	1.37×10^{-4}	$0.44 \times 10^{-4} q_0$	1.15×10^{-4}	$0.36 \times 10^{-4} q_0$
			first run		second run

8.3 Conclusions

In fig. 11, we compare the theoretical predicted strains with the experimental ones. It is easy to see that close to the crack tip the theoretical results are slightly lower than the experimental ones, e.g. there exists an error of about 3% for the first gage. We recall that in the theoretical formula we neglected terms of $O(\lambda^4)$. This fact could contribute to the difference, as well as the averaging effect of the finite gage thickness. As we move further away from the crack tip the theoretical values become smaller than the experimental ones. This is to be expected, since now ϵ is large and the non-singular terms become significant. Our theoretical results were computed on the basis of only the singular term and furthermore only up to terms of $O(\lambda^2)$.

While it should be pointed out that the bending stresses are practically negligible for this particular test configuration, it was found that on the whole the experimental and theoretical results compare very well.

CHAPTER IX
CONCLUSIONS

The local stresses near the crack point are found to be proportional to $1/\sqrt{r}$ which is characteristic for crack problems. Furthermore, the angular distribution around the crack tip is exactly the same as that of a flat sheet, and the curvature appears only in the intensity factors and in such a way that for $R \rightarrow \infty$ we recover the flat sheet behavior. A typical term is

$$\sigma_{shell} \sim \sigma_{plate} \left\{ 1 + \frac{\text{const } c^2}{R^2} + O\left(\frac{1}{R^2}\right) \right\} \quad (8.1)$$

where the constant is a positive quantity. The general effect of initial curvature, in reference to that of a flat sheet, is to increase the stress in the neighborhood of the crack point. Furthermore, it is of some practical value to be able to correlate flat sheet behavior with that of initially curved specimens. In experimental work on brittle fracture for example, considerable time might be saved since by 8.1 we would expect to predict the response behavior of curved sheets from flat sheet tests.

The stresses also indicate that there exists an interaction between bending and stretching, i. e. bending loadings will generally produce both bending and stretching stresses, and vice versa.

It is well known that large, thin-walled pressure vessels resemble balloons and like balloons are subject to puncture and explosive loss. For any given material, under a specified stress field due to internal pressure, there will be a crack length in the material which will be self propagating. Crack lengths less than

the critical value will cause leakage but not destruction. However, if the critical length is ever reached, either by penetration or by the growth of a small fatigue crack, the explosion and complete loss of the structure occurs. This critical crack length, using Griffith's criterion, was shown to depend upon the stress field, the radius and thickness of the vessel, as well as the material itself (see 7.20). We were also able to obtain a relation for the ratio ^{of the} critical crack length of a spherical shell ^{to the} ~~over~~ critical crack length of a flat sheet (see eq. 7.23). In general this ratio is less than unity, which again indicates clearly that a cracked initially curved shell is weaker than a cracked flat sheet subjected to the same loading.

In conclusion it must be emphasized that the classical bending theory has been used in deducing the foregoing results. Hence it is inherent that only the Kirchhoff equivalent shear free condition is satisfied along the crack, and not the vanishing of both individual shearing stresses. While outside the local region the stress distribution should be accurate, one might expect the same type of discrepancy to exist near the crack point as that found by Knowles and Wang [7] in comparing Kirchhoff and Reissner bending results for the flat plate case [8, 9]. In this case the order of the stress singularity remained unchanged but the circumferential distribution around the crack changed so as to be precisely the same as that due to solely extensional loading. Pending further investigation of this effect for initially curved plates, one is tempted to conjecture that the bending amplitude and angular distribution would be the same as that of

stretching.

Finally for a clamped spherical shell, the experimental and theoretical strains ϵ_y , at three different locations along the crack prolongation, compare very well.

APPENDIX I

1. Table of F.C. Transforms:

We list below the following integrals which are useful for the evaluation of the kernels L_1^* , L_2^* , L_3^* , L_4^*

$$\int_0^\infty \frac{e^{-\sqrt{s^2 - \lambda^2 \alpha^2} |y|}}{\sqrt{s^2 - \lambda^2 \alpha^2}} \cos \zeta s ds = K_0(\lambda \rho e) \quad (1)$$

$$\int_0^\infty e^{-\sqrt{s^2 - \lambda^2 \alpha^2} |y|} \cos \zeta s ds = \frac{\lambda \beta |y|}{\rho} K_1(\lambda \rho e) \quad (2)$$

$$-\int_0^\infty \frac{s^2 e^{-\sqrt{s^2 - \lambda^2 \alpha^2} |y|}}{\sqrt{s^2 - \lambda^2 \alpha^2}} \cos \zeta s ds = \frac{\lambda^2 \beta^2 \zeta^2}{\rho^2} K_0(\lambda \rho e) \quad (3)$$

$$+ \frac{\lambda \beta (\zeta^2 - |y|^2)}{\rho^3} K_1(\lambda \rho e)$$

$$-\int_0^\infty \sqrt{s^2 - \lambda^2 \alpha^2} e^{-\sqrt{s^2 - \lambda^2 \alpha^2} |y|} \cos \zeta s ds = \left(\frac{\lambda \beta}{\rho} - \frac{\lambda \beta |y|^2}{\rho^3} \right) K_1(\lambda \rho e) \quad (4)$$

$$+ \frac{\lambda^2 \beta^2 |y|^2}{\rho^2} K_1'(\lambda \rho e)$$

$$\int_0^\infty e^{-|y|s} \cos \zeta s ds = \frac{|y|}{\rho^2} \quad (5)$$

$$\int_0^\infty s e^{-s|y|} \cos \zeta s ds = -\frac{1}{\rho^2} + \frac{2|y|^2}{\rho^4} = \quad (6)$$

$$-\int_0^\infty s \sqrt{s^2 - \lambda^2 \alpha^2} e^{-\sqrt{s^2 - \lambda^2 \alpha^2} |y|} \sin \zeta s ds = \frac{\lambda^2 \beta^2 \zeta}{\rho^4} (\zeta^2 - 3|y|^2) K_2(\lambda \rho e) \quad (7)$$

$$- \frac{\lambda^3 \beta^3 \zeta |y|^2}{\rho^3} K_1(\lambda \rho e)$$

$$-\int_0^{\infty} s^2 \sqrt{s^2 - \lambda^2 \alpha^2} e^{-\sqrt{s^2 - \lambda^2 \alpha^2} |y|} \cos \zeta s ds = -\frac{3\lambda^2 \beta^2}{\rho^5} (\zeta^4 + |y|^4 - 6\zeta^2 |y|^2) K_2(\lambda \rho e) \quad (8)$$

$$-\frac{\lambda^3 \beta^3}{\rho^5} (\zeta^4 + |y|^4 - 4\zeta^2 |y|^2) K_1(\lambda \rho e) + \frac{\lambda^4 \beta^4 \zeta^2 |y|^2}{\rho^4} K_2(\lambda \rho e)$$

2. Table of Proper and Improper Integrals

Another set of integrals which are used in Chapter IV, section 5, are (where $|x| < 1$):

$$\text{C.P.V.} \int_{-1}^1 \frac{\sqrt{1-\xi^2}}{x-\xi} d\xi = \pi x \quad (9)$$

$$\text{C.P.V.} \int_{-1}^1 \frac{(1-\xi^2)^{3/2}}{x-\xi} d\xi = \pi \left(\frac{3}{2} x - x^3 \right) \quad (10)$$

$$\text{C.P.V.} \int_{-1}^1 \frac{(1-\xi^2)^{5/2}}{x-\xi} d\xi = \pi \left(\frac{15}{8} x - \frac{5}{2} x^3 + x^5 \right) \quad (11)$$

$$\int_{-1}^1 \frac{(1-\xi^2)^{7/2}}{x-\xi} d\xi = \pi \left(\frac{35}{16} x - \frac{35}{8} x^3 + \frac{7}{2} x^5 - x^7 \right)$$

$$\int_{-1}^1 \sqrt{1-\xi^2} (x-\xi) \ln \frac{\lambda \alpha |x-\xi|}{2} d\xi = \frac{\pi}{4} \left(1 + \ln \frac{\lambda^2 \alpha^2}{16} \right) x + \frac{\pi}{6} x^3 \quad (12)$$

$$\int_{-1}^1 \sqrt{1-\xi^2} (x-\xi)^3 \ln \frac{\lambda \alpha |x-\xi|}{2} d\xi = \left(\frac{3}{32} - \frac{1}{4} \ln \frac{\lambda \alpha}{4\sqrt{2}} \right) \pi x + \frac{\pi}{4} x^3 - \frac{\pi x^5}{20} \quad (13)$$

To evaluate I2 proceed as follows. First define

$$I(x) \equiv \int_{-1}^1 \sqrt{1-\xi^2} (x-\xi) \ln \left[\frac{\lambda\alpha}{2} |x-\xi| \right] d\xi$$

which is continuous and bounded for all $-1 < x < 1$ and $-1 \leq \xi \leq 1$. Formally, upon differentiation with respect to x

$$\begin{aligned} I'(x) &= \int_{-1}^1 \sqrt{1-\xi^2} \left\{ \ln \left[\frac{\lambda\alpha}{2} |x-\xi| \right] + 1 \right\} d\xi \\ &= \frac{\pi}{2} + \int_{-1}^1 \sqrt{1-\xi^2} \ln \left[\frac{\lambda\alpha}{2} |x-\xi| \right] d\xi \equiv \frac{\pi}{2} + I_1(x) \end{aligned}$$

where

$$I_1(x) \equiv \text{c. P. V} \int_{-1}^1 \sqrt{1-\xi^2} \ln \left[\frac{\lambda\alpha}{2} |x-\xi| \right] d\xi$$

Next differentiating $I_1(x)$ once we obtain

$$I_1'(x) = \int_{-1}^1 \frac{\sqrt{1-\xi^2}}{x-\xi} d\xi = \pi x$$

Integrating once gives

$$I_1(x) = \frac{\pi x^2}{2} + I_1(0)$$

where

$$I_1(0) \equiv \int_{-1}^1 \sqrt{1-\xi^2} \ln \frac{\lambda\alpha|\xi|}{2} d\xi = -\frac{\pi}{4} + \frac{\pi}{2} \ln \frac{\lambda\alpha}{4}$$

and hence

$$I(x) = \frac{\pi}{4} \left[1 + \ln \frac{\lambda^2 \alpha^2}{16} \right] x + \frac{\pi}{6} x^3 + I(0)$$

where

$$I(0) \equiv - \int_{-1}^1 \sqrt{1-\xi^2} \xi \ln \frac{\lambda\alpha|\xi|}{2} d\xi = 0$$

3. Some Integrals of the Bessel Functions $J_1(s)$

Below we list a set of integrals which are used in Chapter IV, section 7.

$$\int_0^{\infty} J_1(s) e^{-s|y|} \cos xs \, ds = \operatorname{Re} \int_0^{\infty} J_1(s) e^{-s[|y|-ix]} \, ds$$

$$= \frac{1}{\sqrt{2\epsilon}} \cos \frac{\theta}{2} + O(\epsilon^0) \quad (14)$$

$$\int_0^{\infty} J_1(s) e^{-s|y|} \sin xs \, ds = -\frac{1}{\sqrt{2\epsilon}} \sin \frac{\theta}{2} + O(\epsilon^0) \quad (15)$$

$$|y| \int_0^{\infty} s J_1(s) e^{-s|y|} \cos xs \, ds = \frac{1}{4\sqrt{2\epsilon}} \left[\cos \frac{\theta}{2} - \cos \frac{5\theta}{2} \right] + O(\epsilon^0) \quad (16)$$

$$|y| \int_0^{\infty} s J_1(s) e^{-s|y|} \sin xs \, ds = -\frac{1}{4\sqrt{2\epsilon}} \left[\sin \frac{\theta}{2} - \sin \frac{5\theta}{2} \right] + O(\epsilon^0) \quad (17)$$

4. Properties of the $K_n(z)$

$$K_0'(z) = -K_1(z) \quad (18)$$

$$K_0''(z) = -K_1'(z) = K_0(z) + \frac{K_1(z)}{z} \quad (19)$$

For small arguments z the expansions are:

$$K_0(z) = -(\gamma + \ln \frac{z}{2}) \left[1 + \left(\frac{z}{2}\right)^2 + \frac{1}{2^2} \left(\frac{z}{2}\right)^4 \right]$$

(20)

$$+ \left(\frac{z}{2}\right)^2 \frac{1}{(1!)^2} + \frac{3}{2} \frac{1}{(2!)^2} \left(\frac{z}{2}\right)^4 + O(z^6 \ln z)$$

$$K_1(z) = \frac{1}{z} + \left(\gamma + \ln \frac{z}{2} \right) \left[\frac{z}{2} + \left(\frac{z}{2} \right)^3 \frac{1}{1^2 \cdot 2} + \left(\frac{z}{2} \right)^5 \frac{1}{1^2 \cdot 2^2 \cdot 3} \right]$$

(21)

$$-\frac{1}{2} \left(\frac{z}{2} \right) - \frac{5}{4 \cdot 2!} \left(\frac{z}{2} \right)^3 - \frac{10}{6} \frac{1}{2! 3!} \left(\frac{z}{2} \right)^5 + O(z^7 \ln z).$$

APPENDIX II

On the Solution of Singular Integral Equations

For simplicity, we will consider the case of a single singular integral equation of the type encountered in Chapter III, sect. 5, i. e.

$$\int_{-1}^1 \left\{ \frac{1}{x-\xi} + \lambda^2 g(x, \xi) \right\} u(\xi) d\xi = m_0 x \quad ; \quad |x| < 1 \quad (1)$$

where $g(x, \xi)$ is continuous and bounded for all x and ξ and furthermore symmetric, i. e. $g(x, \xi) = g(\xi, x)$ and $g(x, x) = 0$. Equation 1 can be written in the form

$$\int_{-1}^1 \frac{u(\xi)}{x-\xi} d\xi = f(x) \quad (2)$$

where

$$f(x) = m_0 x - \lambda^2 \int_{-1}^1 g(x, \xi) u(\xi) d\xi \quad (3)$$

We next seek a solution to equation 2 such that it is bounded $[-1, 1]$ and is Hölder continuous for some positive Hölder index μ .

Following Muskhelishvili [6] §47, the solution can be written in the form:

$$u(x) = \frac{1}{\pi^2} \sqrt{\frac{1+x}{1-x}} \int_{-1}^1 \sqrt{\frac{1-t}{1+t}} \frac{f(t)}{t-x} dt \quad (4)$$

or substituting for $f(t)$

$$u(x) = \frac{1}{\pi^2} \sqrt{\frac{1+x}{1-x}} \left\{ \int_{-1}^1 \sqrt{\frac{1-t}{1+t}} \frac{m_0 t}{t-x} dt \right. \quad (5)$$

$$\left. - \lambda^2 \int_{-1}^1 \sqrt{\frac{1-t}{1+t}} \int_{-1}^1 g(t, \xi) u(\xi) \frac{d\xi}{t-x} dt \right.$$

which after some rearrangement can be written in the form:

$$u(x) + \frac{\lambda^2}{\pi^2} \sqrt{\frac{1+x}{1-x}} \int_{-1}^1 \frac{1-t}{1+t} \frac{dt}{x-t} \int_{-1}^1 g(t, \xi) u(\xi) d\xi = \frac{m_0}{\pi} \sqrt{1-x^2} \quad (6)$$

Using the Poincaré-Betrand transformation formula we find

$$\begin{aligned} \sqrt{\frac{1+x}{1-x}} \int_{-1}^1 \frac{1-t}{1+t} \frac{dt}{t-x} \int_{-1}^1 g(t, \xi) u(\xi) d\xi &= \sqrt{\frac{1+x}{1-x}} \int_{-1}^1 u(\xi) \int_{-1}^1 \frac{1-t}{1+t} \frac{g(t, \xi)}{t-x} dt d\xi \\ &= \int_{-1}^1 u(\xi) K(x, \xi) d\xi \end{aligned}$$

which substituted in 6 will give

$$u(x) + \frac{\lambda^2}{\pi^2} \int_{-1}^1 u(\xi) K(x, \xi) d\xi = \frac{m_0}{\pi} \sqrt{1-x^2} \quad (7)$$

i. e. we have reduced the singular integral equation 1 to a Fredholm integral equation of the second kind, where the kernel $K(x, \xi)$ is a continuous and bounded function of x and ξ .

We will now seek the solution of the integral equation

$$u(x) = \frac{m_0}{\pi} \sqrt{1-x^2} - \frac{\lambda^2}{\pi^2} \int_{-1}^1 u(\xi) K(x, \xi) d\xi \quad (8)$$

by the method of successive approximations. For the zero-order approximation let us take the right-hand side of equation 8 namely

$$u_0(x) = \frac{m_0}{\pi} \sqrt{1-x^2} \quad (9)$$

substitute into 8 to obtain

$$\begin{aligned}
 u_1(x) &= \frac{m_0}{\pi} \sqrt{1-x^2} - \frac{m_0 \lambda^2}{\pi^3} \int_{-1}^1 K(x, \xi) \sqrt{1-\xi^2} d\xi \\
 &= \frac{m_0}{\pi} \sqrt{1-x^2} - \frac{m_0 \lambda^2}{\pi} \sqrt{\frac{1+x}{1-x}} \int_{-1}^1 \sqrt{\frac{1-t}{1+t}} \frac{dt}{t-x} \int_{-1}^1 \sqrt{1-\xi^2} g(t, \xi) d\xi
 \end{aligned} \tag{10}$$

and in general

$$u_N(x) = \frac{m_0}{\pi} \sqrt{1-x^2} - \frac{m_0}{\pi} \sum_{n=1}^N \frac{\lambda^{2n}}{\pi^{2n}} \int_{-1}^1 K_{(n)}(x, \xi) \sqrt{1-\xi^2} d\xi \tag{11}$$

where $K_{(n)}(x, \xi)$ is determined from the recurrence relationship

$$K_{(0)}(x, \xi) = K(x, \xi) \quad ; \quad K_{(n)}(x, \xi) = \int_{-1}^1 K(x, t) K_{(n-1)}(t, \xi) dt \tag{12}$$

Assuming that the successive approximations do converge, and proceeding to the limit in equation 11 we obtain a solution of the integral equation 7 in the form of an infinite series

$$u(x) = \frac{m_0}{\pi} \sqrt{1-x^2} - \frac{m_0}{\pi} \sum_{n=1}^{\infty} \left(\frac{\lambda}{\pi}\right)^{2n} \int_{-1}^1 K_n(x, \xi) \sqrt{1-\xi^2} d\xi \tag{13}$$

These successive approximations do converge uniformly for all values of λ lying inside the circle $|\lambda|^2 \leq \frac{1}{B}$, where*

$$\begin{aligned}
 B^2 &= \frac{1}{\pi^4} \int_{-1}^1 \int_{-1}^1 |K(x, \xi)|^2 dx d\xi \\
 &= \frac{1}{\pi^4} \int_{-1}^1 \int_{-1}^1 \left| \sqrt{\frac{1+x}{1-x}} \int_{-1}^1 \sqrt{\frac{1-t}{1+t}} \frac{g(t, \xi)}{t-x} dt \right|^2 dx d\xi
 \end{aligned}$$

* If the kernel is also a function of λ , then $B = B(\lambda)$ and therefore the solution of the inequality

$$|\lambda|^2 \leq \frac{1}{B(\lambda)}$$

will give us the radius of convergence.

The limit of the successive approximations is the solution of equation 7 and this solution is unique.* Furthermore, if in the series 13 only those terms are included which contain powers of λ up to the $2n$ -th, then the magnitude of the error will not exceed

$$D \sqrt{C_1} \frac{|\lambda|^{2n+2} B^n}{1 - \lambda^2 B}$$

In particular if

$$g(x, \xi) = g(x-\xi) \equiv g(\zeta) = -\frac{2}{\lambda^2 \beta^2} \left\{ -\frac{\lambda^2 \beta^2}{\zeta} K_0(\lambda \beta |\zeta|) - \left(\lambda^3 \beta^3 \frac{\zeta}{|\zeta|^3} + \frac{2\lambda\beta}{\zeta |\zeta|} \right) K_1(\lambda \beta |\zeta|) + \frac{2}{\zeta^3} \right\} - \frac{1}{\zeta} \quad (14)$$

which when expanded for small arguments gives

$$g(x, \xi) = -2\beta^2(x-\xi) \left[\frac{5}{32} - \frac{3\lambda}{8} - \frac{3}{8} \ln \frac{\lambda\beta|x-\xi|}{2} \right] + O(\lambda^2(x-\xi)^3 \ln \lambda|x-\xi|) \quad (15)$$

and therefore the integrals

$$\begin{aligned} I_1(t) &\equiv \int_{-1}^1 \sqrt{1-\xi^2} g(t, \xi) d\xi = \\ &= -2\beta^2 \left[\left(\frac{5}{32} - \frac{3\lambda}{8} \right) \frac{\pi}{2} - \frac{3\pi}{32} \left(1 + \ln \frac{\lambda^2 \beta^2}{16} \right) t + \frac{\beta^2}{8} \pi t^3 + O(\lambda^2) \right] \\ &\equiv C_1 t + 2C_2 t^3 + O(\lambda^2) \end{aligned} \quad (16)$$

* For a proof of this theorem see Mikhlin [14], pp. 7-13.

$$\begin{aligned}
 I_2 &\equiv \int_{-1}^1 \sqrt{\frac{1-t}{1+t}} \frac{I_1(t)}{t-x} dt \\
 &= c_1 \int_{-1}^1 \sqrt{\frac{1-t}{1+t}} \frac{t}{t-x} dt + 2c_2 \int_{-1}^1 \sqrt{\frac{1-t}{1+t}} \frac{t^3}{t-x} dt + o(\lambda^2) \\
 &= c_1 \pi(1-x) + c_2 \pi(1-x)(1+2x^2) + o(\lambda^2) \\
 &= \pi(1-x) [c_1 + c_2(1+2x^2)] + o(\lambda^2) \tag{17}
 \end{aligned}$$

from which

$$\begin{aligned}
 u_1(x) &= \frac{m_0}{\pi} \sqrt{1-x^2} - \frac{m_0 \lambda^2}{\pi^2} \sqrt{1-x^2} [c_1 + c_2(1+2x^2)] + o(\lambda^2) \\
 &= \frac{m_0}{\pi} \sqrt{1-x^2} \left\{ 1 - \frac{1}{\pi} [c_1 + c_2(1+2x^2)] \lambda^2 + o(\lambda^2) \right\} \\
 &= \frac{m_0}{\pi} \sqrt{1-x^2} \left\{ 1 - \frac{c_1 \lambda^2}{\pi} - \frac{3}{\pi} c_2 \lambda^2 + \frac{2}{\pi} c_2 \lambda^2 (1-x^2) + o(\lambda^2) \right\} \\
 &= -m_0 \sqrt{1-x^2} \left\{ A_1 + A_2 (1-x^2) + o(\lambda^2) \right\} \tag{18}
 \end{aligned}$$

where

$$A_1 = 1 - \lambda^2 \beta^2 \left[\frac{7}{32} + \frac{3\beta}{8} + \frac{3}{16} \ln \frac{\lambda^2 \beta^2}{16} \right] + o(\lambda^4) \tag{19}$$

$$A_2 = \frac{\lambda^2 \beta^2}{8} + o(\lambda^4) \tag{20}$$

Next we will show that if in equation 1 we assume a power series solution of the form:

$$u_1(x) = \sqrt{1-x^2} \left\{ A_1^* + \lambda^2 A_2^* (1-x^2) + \dots \right\} \quad (21)$$

the coefficients will be identical to the ones obtained by the previous method, which indicates that the two methods are equivalent. Substituting 21 into 1, integrating and equating coefficients on both sides of the resulting equation, it is easy to show that $A_1^* = A_1$ and so on. In a similar fashion this can be carried out for coupled integral equations. In Chapter IV we encountered two coupled integrals of the form:

$$\int_{-1}^1 \frac{u_1(\xi) - u_2(\xi)}{x - \xi} d\xi = m_0 x - \lambda^2 \int_{-1}^1 g_{11}(x, \xi) u_1(\xi) d\xi - \lambda^2 \int_{-1}^1 g_{12}(x, \xi) u_2(\xi) d\xi ; |x| < 1 \quad (22)$$

$$\int_{-1}^1 \frac{u_1(\xi) + u_2(\xi)}{x - \xi} d\xi = \tilde{m}_0 x - \lambda^2 \int_{-1}^1 g_{21}(x, \xi) u_1(\xi) d\xi - \lambda^2 \int_{-1}^1 g_{22}(x, \xi) u_2(\xi) d\xi ; |x| < 1 \quad (23)$$

where the functions $g_{ik}(x, \xi)$ ($i, k = 1, 2$) are to be continuous and bounded for all x and ξ in the interval $[1, -1]$.

For convenience we define

$$f_1(x) = m_0 x - \lambda^2 \int_{-1}^1 g_{11}(x, \xi) u_1(\xi) d\xi - \lambda^2 \int_{-1}^1 g_{12}(x, \xi) u_2(\xi) d\xi \quad (24)$$

$$f_2(x) = \tilde{m}_0 x - \lambda^2 \int_{-1}^1 g_{21}(x, \xi) u_1(\xi) d\xi - \lambda^2 \int_{-1}^1 g_{22}(x, \xi) u_2(\xi) d\xi \quad (25)$$

Thus equations 22 and 23 can be written in the form

$$\int_{-1}^1 \frac{u_1(\xi) - u_2(\xi)}{x - \xi} d\xi = f_1(x) \quad (26)$$

$$\int_{-1}^1 \frac{u_1(\xi) + u_2(\xi)}{x - \xi} d\xi = f_2(x) \quad (27)$$

We seek for solutions to the system such that they are bounded in $[-1, 1]$ and are Hölder continuous for some positive Hölder indices μ_1 and μ_2 . Again following Muskhelishvili [6] the solutions can be written in the form

$$u_1(x) - u_2(x) = \frac{1}{\pi^2} \sqrt{\frac{1+x}{1-x}} \int_{-1}^1 \sqrt{\frac{1-t}{1+t}} \frac{f_1(t)}{t-x} dt \quad (28)$$

$$u_1(x) + u_2(x) = \frac{1}{\pi^2} \sqrt{\frac{1+x}{1-x}} \int_{-1}^1 \sqrt{\frac{1-t}{1+t}} \frac{f_2(t)}{t-x} dt \quad (29)$$

Substituting for $f_1(t)$ and $f_2(t)$ and integrating the following equations result

$$u_1(x) - u_2(x) = \frac{m_0}{\pi} \sqrt{1-x^2} - \frac{\lambda^2}{\pi^2} \sqrt{\frac{1+x}{1-x}} \int_{-1}^1 \sqrt{\frac{1-t}{1+t}} \left\{ \int_{-1}^1 g_{10}(t, \xi) u_1(\xi) d\xi + \int_{-1}^1 g_{12}(t, \xi) u_2(\xi) d\xi \right\} \frac{dt}{t-x} \quad (30)$$

$$u_1(x) + u_2(x) = \frac{\tilde{m}_0}{\pi} \sqrt{1-x^2} - \frac{\lambda^2}{\pi^2} \sqrt{\frac{1+x}{1-x}} \int_{-1}^1 \sqrt{\frac{1-t}{1+t}} \left\{ \int_{-1}^1 g_{21}(t, \xi) u_1(\xi) d\xi + \int_{-1}^1 g_{22}(t, \xi) u_2(\xi) d\xi \right\} \frac{dt}{t-x} \quad (31)$$

We thus have reduced our problem to the solution of two Fredholm integral equations the solutions of which we will seek by the method of successive approximations. As before for a zero-order approximation let us take the right-hand side of equations 30 and 31, i.e.

$$u_{10}(x) - u_{20}(x) = \frac{m_0}{\pi} \sqrt{1-x^2} \quad (32)$$

$$u_{10}(x) + u_{20}(x) = \frac{\tilde{m}_0}{\pi} \sqrt{1-x^2} \quad (33)$$

and so on. The theory, and likewise the method of solution, of systems of integral equations, are just the same as for a single equation. Thus successive approximations converge for small λ and in particular if λ satisfies the inequality (see ref. [14], pp. 30-31)

$$\lambda^2 \leq \lambda^{*2} < \left\{ \max_{1 \leq i \leq n} \sum_{k=1}^2 \sqrt{\int_{-1}^1 \int_{-1}^1 |K_{ik}(x,s)|^2 dx ds} \right\}^{-1}$$

where

$$K_{ik}(x,s) \equiv \frac{1}{\pi^2} \sqrt{\frac{1+x}{1-x}} \int_{-1}^1 \sqrt{\frac{1-\xi}{1+\xi}} g_{ik}(s,\xi) u_k(\xi) \frac{d\xi}{x-\xi}$$

In our particular example the functions g_{ik} are of the form:

$$g_{11}(x,\xi) = g_{11}(x-\xi) \equiv g_{11}(\xi) = -\frac{2}{\lambda^2 \beta^2} \left\{ -\frac{\lambda^2 \beta^2}{\xi} K_0(\lambda \beta |\xi|) - \right. \\ \left. - \left(\lambda^3 \beta^3 \frac{\xi}{|\xi|} + \frac{2\lambda\beta}{\xi|\xi|} \right) K_1(\lambda \beta |\xi|) + \frac{2}{\xi^3} \right\} - \frac{1}{\xi} \quad (34)$$

$$g_{12}(x, \xi) = g_{11}(x - \xi) \equiv g_{11}(\xi) \equiv -\frac{2}{\lambda^2 \alpha^2} \left\{ -\frac{\lambda^2 \alpha^2}{\xi} K_0(\lambda \alpha |\xi|) \right. \\ \left. - \left(\lambda^3 \alpha^3 \frac{\xi}{|\xi|} + \frac{2\lambda \alpha}{\xi |\xi|} \right) K_1(\lambda \alpha |\xi|) + \frac{2}{\xi^3} \right\} - \frac{1}{\xi} \quad (35)$$

$$g_{21}(x, \xi) = g_{21}(x - \xi) \equiv g_{21}(\xi) = -\frac{2}{\lambda^2 \beta^2 (1 - \nu_0)} \left\{ -\frac{\nu_0 \lambda^2 \beta^2}{\xi} K_0(\lambda \beta |\xi|) - \nu_0 \left(\lambda^3 \beta^3 \frac{\xi}{|\xi|} + \frac{2\lambda \beta}{\xi |\xi|} + \frac{2\lambda \beta}{\xi |\xi|} \right) \right. \\ \left. K_1(\lambda \beta |\xi|) - \alpha^2 \beta \lambda^2 \frac{\xi}{|\xi|} K_1(\lambda \beta |\xi|) + \frac{2\nu_0}{\xi^3} - \frac{\alpha^2 \lambda^2}{\xi} \right\} - \frac{1}{\xi} \quad (36)$$

$$g_{22}(x, \xi) = g_{22}(x - \xi) \equiv g_{22}(\xi) = -\frac{2}{\lambda^2 \alpha^2 (1 - \nu_0)} \left\{ -\frac{\nu_0 \lambda^2 \alpha^2}{\xi} K_0(\lambda \alpha |\xi|) - \nu_0 \left(\lambda^3 \alpha^3 \frac{\xi}{|\xi|} + \frac{2\lambda \alpha}{\xi |\xi|} + \frac{2\lambda \alpha}{\xi |\xi|} \right) \right. \\ \left. K_1(\lambda \alpha |\xi|) - \alpha \beta^2 \lambda^2 \frac{\xi}{|\xi|} K_1(\lambda \alpha |\xi|) + \frac{2\nu_0}{\xi^3} - \frac{\beta^2 \lambda^2}{\xi} \right\} - \frac{1}{\xi} \quad (37)$$

The successive approximations follow the same pattern as for the single integral equation. It is an easy matter to show that the coefficients obtained are identical to those obtained by the method employed in sect. 5, Chapter IV. This therefore establishes the equivalence of the two methods.

APPENDIX III

Some Details for the Antisymmetric Problem

1. Case of $v_0 = 0, t_0 \neq 0$:

Following exactly the same method as in Chapter IV we list below the successive steps:

$$Q_2 = - (Q_5 - Q_6)$$

$$v_0 s^2 Q_7 = - \left\{ (v_0 s^2 - i\lambda^2) Q_5 + (v_0 s^2 + i\lambda^2) Q_6 \right\}$$

The continuity conditions are satisfied if we take

$$\int_0^{\infty} \frac{Q_5}{s} \cos xs \, ds = 0 \quad ; \quad |x| > 1$$

$$\int_0^{\infty} \frac{Q_6}{s} \cos xs \, ds = 0 \quad ; \quad |x| > 1$$

which by inversion give:

$$Q_5 = \frac{2s}{\pi} \int_0^1 u_3(\xi) \cos \xi s \, d\xi$$

$$Q_6 = \frac{2s}{\pi} \int_0^1 u_4(\xi) \cos \xi s \, d\xi$$

where

$$u_5(x) = \int_0^1 \frac{Q_5}{s} \cos xs \, ds \quad ; \quad |x| < 1$$

$$u_6(x) = \int_0^1 \frac{Q_6}{s} \cos xs \, ds \quad ; \quad |x| < 1$$

In view of the above the corresponding singular integral equations to be solved are:

$$-\frac{i\lambda^2 R D}{\pi c^2} \int_{-1}^1 \left\{ u_3(\xi) M_1 - M_2 u_4(\xi) \right\} d\xi = -t_0 x \quad ; \quad |x| < 1$$

$$\frac{1}{\pi} \int_{-1}^1 \left\{ u_3(\xi) M_3 + u_4(\xi) M_4 \right\} d\xi = 0 \quad ; \quad |x| < 1$$

where the kernels M_1, M_2, M_3, M_4 are defined by

$$M_1 = -\frac{\lambda\beta}{\zeta|\zeta|} K_1(\lambda\beta|\zeta|) + \frac{\lambda^2\beta^2}{\zeta} K_1'(\lambda\beta|\zeta|) + \frac{2}{\zeta^3}$$

$$M_2 = -\frac{\lambda\alpha}{\zeta|\zeta|} K_1(\lambda\alpha|\zeta|) + \frac{\lambda^2\alpha^2}{\zeta} K_1'(\lambda\alpha|\zeta|) + \frac{2}{\zeta^3}$$

$$M_3 = \frac{\alpha^2\beta\lambda^3}{|\zeta|} K_1(\lambda\beta|\zeta|) + \frac{6\nu_0}{\zeta^4} + \frac{\alpha^2\lambda^2}{\zeta^2} - \frac{6\nu_0\lambda\beta}{\zeta^2|\zeta|} K_1(\lambda\beta|\zeta|) \\ - \frac{3\nu_0\lambda^2\beta^2}{\zeta^2} K_0(\lambda\beta|\zeta|) - \frac{\nu_0\lambda^3\beta^3}{|\zeta|} K_1(\lambda\beta|\zeta|)$$

$$M_4 = \frac{\alpha\beta^2\lambda^3}{|\zeta|} K_1(\lambda\alpha|\zeta|) + \frac{6\nu_0}{\zeta^4} + \frac{\beta^2\lambda^2}{\zeta} - \frac{6\nu_0\lambda\alpha}{\zeta^2|\zeta|} K_1(\lambda\alpha|\zeta|) \\ - \frac{3\nu_0\lambda^2\alpha^2}{\zeta^2} K_0(\lambda\alpha|\zeta|) - \frac{\nu_0\lambda^3\alpha^3}{|\zeta|} K_1(\lambda\alpha|\zeta|)$$

which for small arguments can be expanded as:

$$M_1 = \frac{\lambda^2\beta^2}{2\zeta} + \frac{3}{32} \lambda^4\zeta - \frac{\lambda^4\zeta}{8} (\gamma + \ln \frac{\lambda\beta|\zeta|}{2}) + O(\lambda^6 \zeta^3 \ln \lambda|\zeta|)$$

$$M_2 = \frac{\lambda^2\alpha^2}{2\zeta} + \frac{3}{32} \lambda^4\zeta - \frac{\lambda^4\zeta}{8} (\gamma + \ln \frac{\lambda\alpha|\zeta|}{2}) + O(\lambda^6 \zeta^3 \ln \lambda|\zeta|)$$

$$M_3 = -\frac{\nu_0\lambda^2\beta^2}{2\zeta} - \frac{3\lambda^4(8+\nu_0)}{32} \zeta + \frac{\lambda^4\zeta}{8} (4+\nu_0) (\gamma + \ln \frac{\lambda\beta|\zeta|}{2}) + O(\lambda^6 \zeta^3 \ln \lambda|\zeta|)$$

$$M_4 = -\frac{\nu_0\lambda^2\alpha^2}{2\zeta} - \frac{3\lambda^4(8+\nu_0)}{32} \zeta + \frac{\lambda^4\zeta}{8} (4+\nu_0) (\gamma + \ln \frac{\lambda\alpha|\zeta|}{2}) + O(\lambda^6 \zeta^3 \ln \lambda|\zeta|)$$

Following the same method of solution as before we obtain

$$u_3(x) = \sqrt{1-x^2} \sum_{n=1}^{\infty} \tilde{A}_n \lambda^{2n} (1-x^2)^n$$

$$u_4(x) = \sqrt{1-x^2} \sum_{n=1}^{\infty} \tilde{B}_n \lambda^{2n} (1-x^2)^n$$

where again we find:

$$\tilde{A}_1 + \tilde{B}_1 = \frac{2t_0 c^2}{\lambda^4 R D} \left\{ 1 + \frac{\pi \lambda^2}{32} + O(\lambda^4) \right\}$$

$$\tilde{A}_1 - \tilde{B}_1 = \frac{t_0 c^2 \alpha^2}{\lambda^2 R D} \left\{ \frac{\nu_0 - 8 + 4(4 + \nu_0)\gamma}{16\nu_0} + \frac{4 + \nu_0}{8\nu_0} \ln \frac{\lambda^2}{16} + O(\lambda^2 \ln \lambda) \right\}$$

2. Case of $\nu_0 \neq 0, t_0 = 0$

To clarify the point made in the beginning of sect. 1, Chapter V, we elaborate. The integral representations for $\nu_0 \neq 0$ and $t_0 = 0$ are

$$W = \mp \int_0^{\infty} \left\{ Q_1 e^{-\sqrt{s^2 - i\lambda^2}|y|} + Q_2 e^{-\sqrt{s^2 + i\lambda^2}|y|} + Q_3 e^{-s|y|} \right\} \cos xs ds$$

$$F = \mp \frac{i\lambda^2 R D}{c^2} \int_0^{\infty} \left\{ Q_1 e^{-\sqrt{s^2 - i\lambda^2}|y|} - Q_2 e^{-\sqrt{s^2 + i\lambda^2}|y|} + Q_4 e^{-s|y|} \right\} \cos xs ds$$

Again following the same method we list below the successive steps:

$$Q_4 = - (Q_1 - Q_2)$$

$$\nu_0 s^2 Q_3 = - \left\{ (\nu_0 s^2 - i\lambda^2) Q_1 + (\nu_0 s^2 + i\lambda^2) Q_2 \right\}$$

The continuity equations are satisfied if we take

$$\int_0^{\infty} \frac{Q_1}{s^2} \cos xs ds = 0 \quad ; \quad |x| > 1$$

$$\int_0^{\infty} \frac{Q_2}{s^2} \cos xs ds = 0 \quad ; \quad |x| > 1$$

which by inversion give:

$$Q_1 = \frac{2s^2}{\pi} \int_0^1 \tilde{u}_1(\xi) \cos \xi s \, d\xi$$

$$Q_2 = \frac{2s^2}{\pi} \int_0^1 \tilde{u}_2(\xi) \cos \xi s \, d\xi$$

In view of the above the corresponding singular integral equations to be solved are:

$$\frac{2i\lambda^2 R D}{\pi c^2} \int_{-1}^1 \{ \tilde{u}_1 L_1 - \tilde{u}_2 L_2 \} d\xi = 0 \quad ; |x| < 1$$

$$- \frac{2}{\pi} \int_{-1}^1 \{ \tilde{u}_1 L_3 + \tilde{u}_2 L_4 \} d\xi = v_0 \quad ; |x| < 1$$

where

$$2 L_1 \equiv \int_0^\infty \left\{ s^3 \sqrt{s^2 - \alpha^2 \lambda^2} e^{-\sqrt{s^2 - \lambda^2 \alpha^2} |y|} - s^4 e^{-s|y|} \right\} \sin(x-\xi) s \, ds$$

$$2 L_2 \equiv \int_0^\infty \left\{ s^3 \sqrt{s^2 - \beta^2 \lambda^2} e^{-\sqrt{s^2 - \lambda^2 \beta^2} |y|} - s^4 e^{-s|y|} \right\} \sin(x-\xi) s \, ds$$

$$2 L_3 \equiv \int_0^\infty \left\{ (\gamma_0 s^2 + i\lambda^2) \sqrt{s^2 - i\lambda^2} s^2 e^{-\sqrt{s^2 - i\lambda^2} |y|} - s^3 (\gamma_0 s^2 - i\lambda^2) e^{-s|y|} \right\} \cos(x-\xi) s \, ds$$

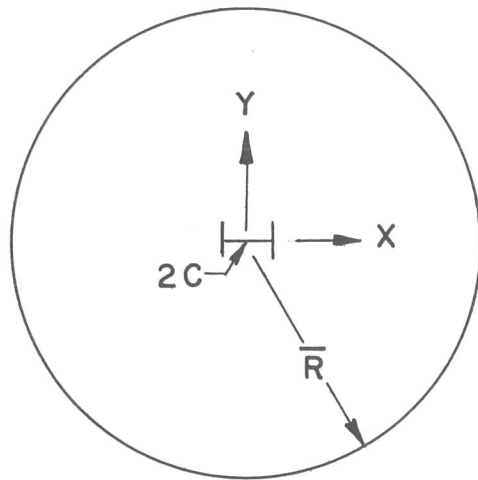
$$2 L_4 \equiv \int_0^\infty \left\{ (\gamma_0 s^2 - i\lambda^2) \sqrt{s^2 + i\lambda^2} s^2 e^{-\sqrt{s^2 + i\lambda^2} |y|} - s^3 (\gamma_0 s^2 + i\lambda^2) e^{-s|y|} \right\} \cos(x-\xi) s \, ds$$

Next we must write the kernels L_1 and L_2 in the form $\frac{\partial^2}{\partial x^2} \{ \Phi, |y| \}$ and then take the limit as $|y| \rightarrow 0$ to recover the required singularity $\frac{1}{x-\xi}$. Unfortunately, we are unable to find this function $\Phi(x, |y|)$ in a closed form.

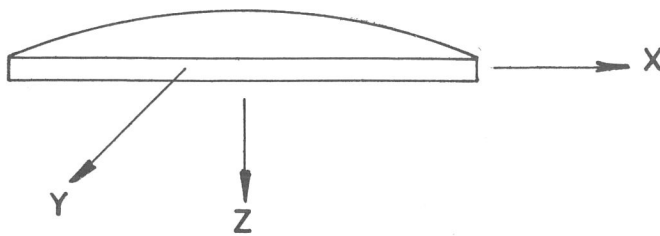
REFERENCES

- [1] Ang, D. D. and Williams, M. L. "Combined Stresses in an Orthotropic Plate Having a Finite Crack." GALCIT SM 60-1, California Institute of Technology, January 1960.
- [2] Reissner, E. "On Some Problems in Shell Theory." Structural Mechanics, Proceedings of the First Symposium on Naval Structural Mechanics. Aug. 11-14, 1958, pp. 74-113.
- [3] Reissner, E. "A Note on Membrane and Bending Stresses in Spherical Shells." F Soc. Industr. Appl. Math. vol. 4, pp. 230-240, 1956.
- [4] Erdelyi, etc. "Tables of Integral Transforms." Vol. 1, Bateman Manuscript Project, 1954, McGraw-Hill, N.Y.
- [5] Noble, B. "The Approximate Solution of Dual Integral Equations by Variational Methods." Proceedings Edinburgh Mathematical Society (1958-59), vol. 11, pp. 113-126.
- [6] Muskhelishvili, N. I. "Singular Integral Equations." English translation by J. R. M. Radok, published by P. Nordhoff, Ltd., Groningen 1953.
- [7] Knowles, J. K. and Wang, N. M. "On the Bending of an Elastic Plate Containing a Crack." Journal of Mathematics and Physics, vol. 39, 1960, pp. 223-236.
- [8] Williams, M. L. "The Bending Stress Distribution at the Base of a Stationary Crack." Journal of Applied Mechanics, vol. 28. Trans. ASME, vol. 83, Series E, 1961, pp. 78-82.

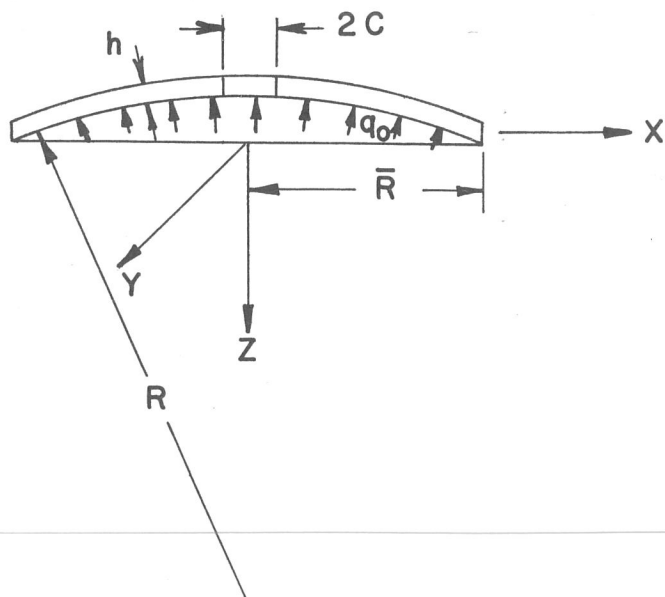
- [9] Williams, M. L. "On the Stress Distribution at the Base of a Stationary Crack." *Journal of Applied Mechanics*, March 1957.
- [10] Reissner, E. "Stresses and Small Displacements of Shallow Spherical Shells I, II" *Journal of Mathematics and Physics* volume 25, 1946, pp. 80-85, 279-300.
- [11] Griffith, A. A. "The Theory of Rupture." *Proceedings of the First International Congress of Applied Mechanics*, Delft, 1924, p. 55.
- [12] Swedlow, J. L. "On Griffith's Theory of Fracture." *GALCIT SM 63-8*, March 29, 1963.
- [13] Parmerter, R. R. "The Buckling of Clamped Shallow Spherical Shells Under Uniform Pressure." September 1963 Ph.D. Dissertation, California Institute of Technology.
- [14] Mikhlin, S. G. "Integral Equations." English translation by A. H. Armstrong, published by Pergamon Press, 1957.



TOP VIEW



SIDE VIEW



CROSS SECTION

FIG. 1 *FINO*

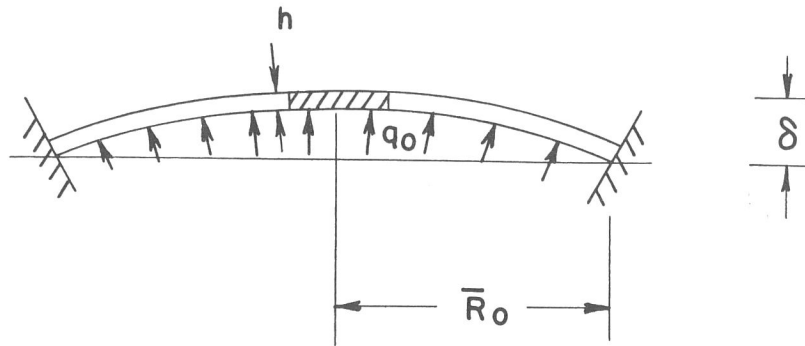


FIG. 2

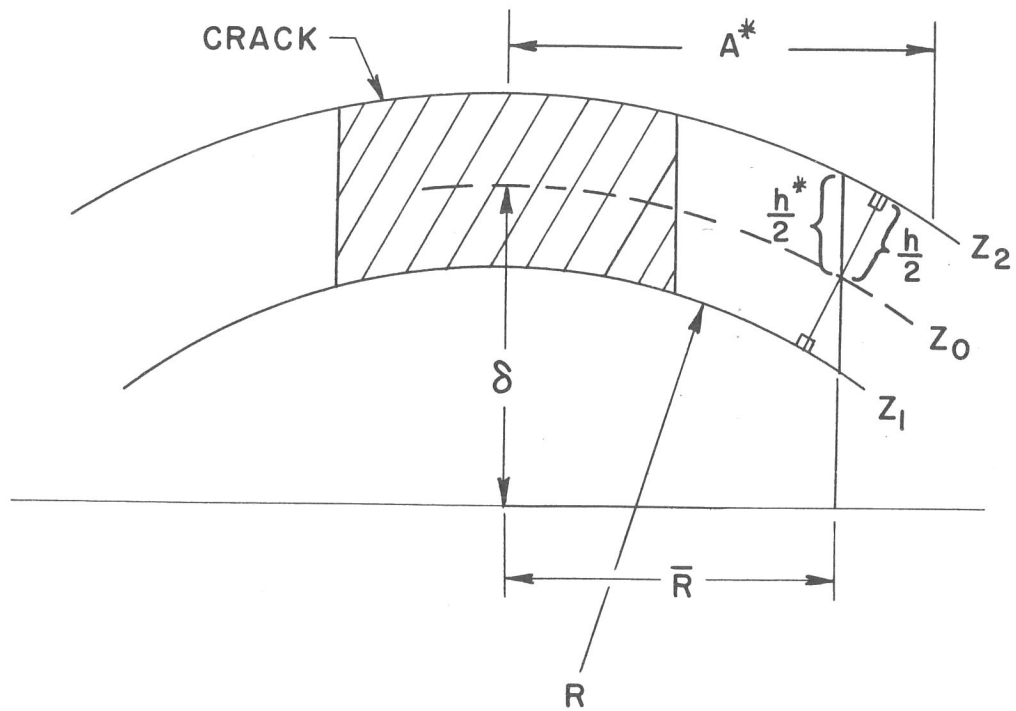


FIG. 3

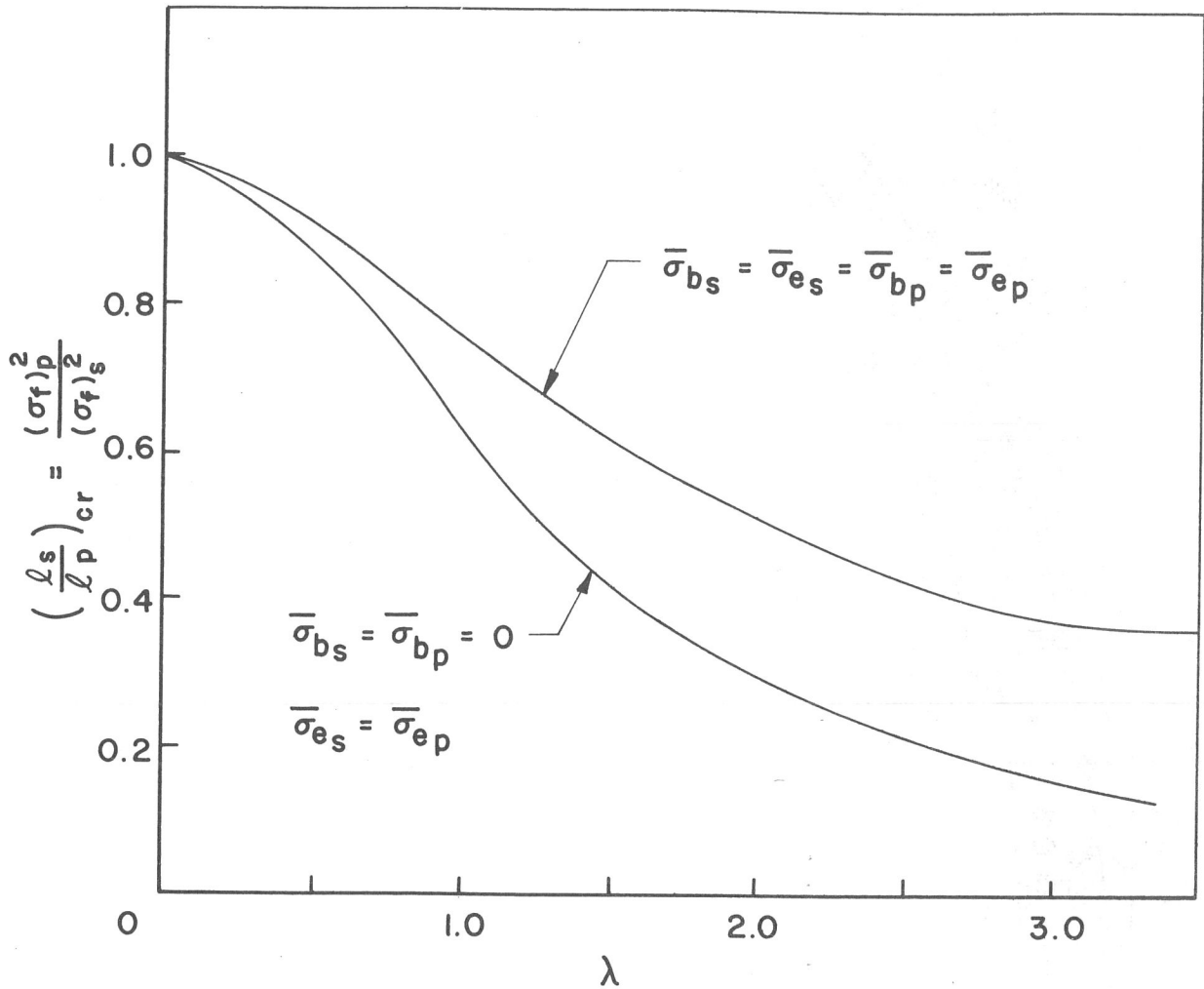


FIG. 4 - RATIO OF CRITICAL CRACK LENGTHS IN A SPHERICAL SHELL AND IN A PLATE VS.

$$\lambda \equiv \sqrt[4]{\frac{12(1-\nu^2)}{R^2 h^2}} c \text{ FOR } \nu = \frac{1}{3}$$

in view of the correction for eq. (7.26) curves should shift a little to the right, same trend.

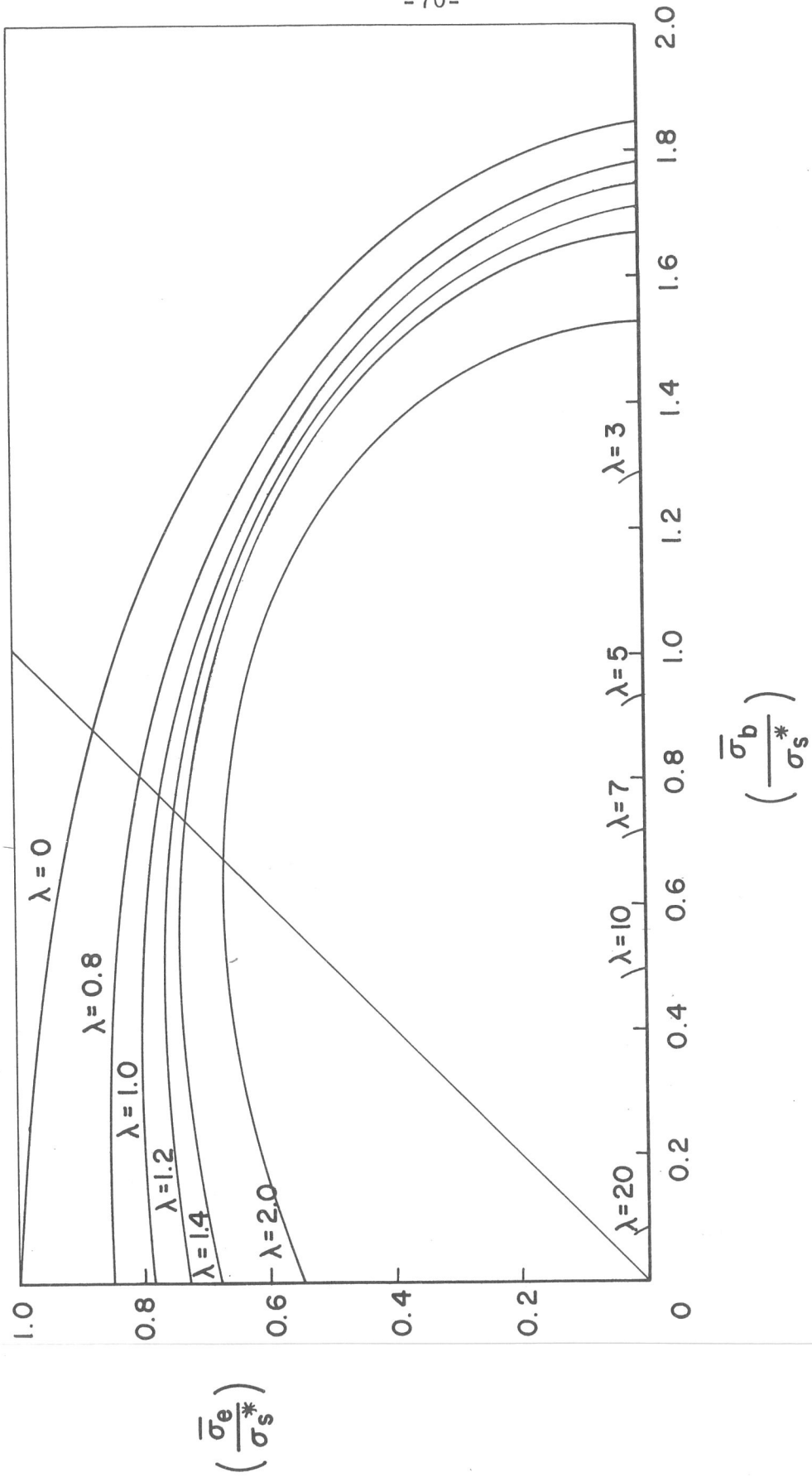


FIG. 5 - INTERACTION CURVES BETWEEN STRETCHING AND BENDING FOR VARIOUS λ AND $\nu = 1/3$

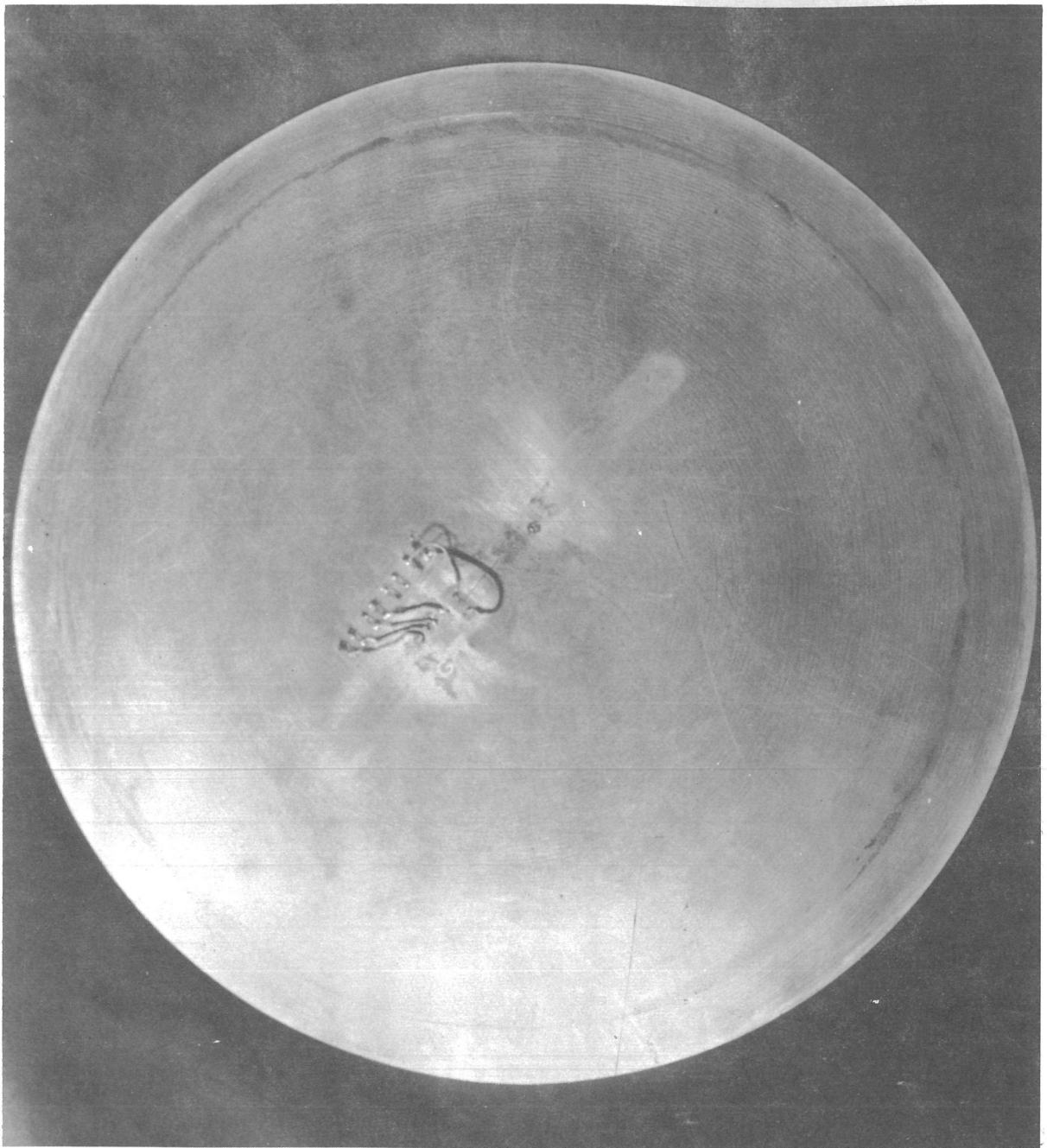


Fig. 6. Photograph of shell after testing.

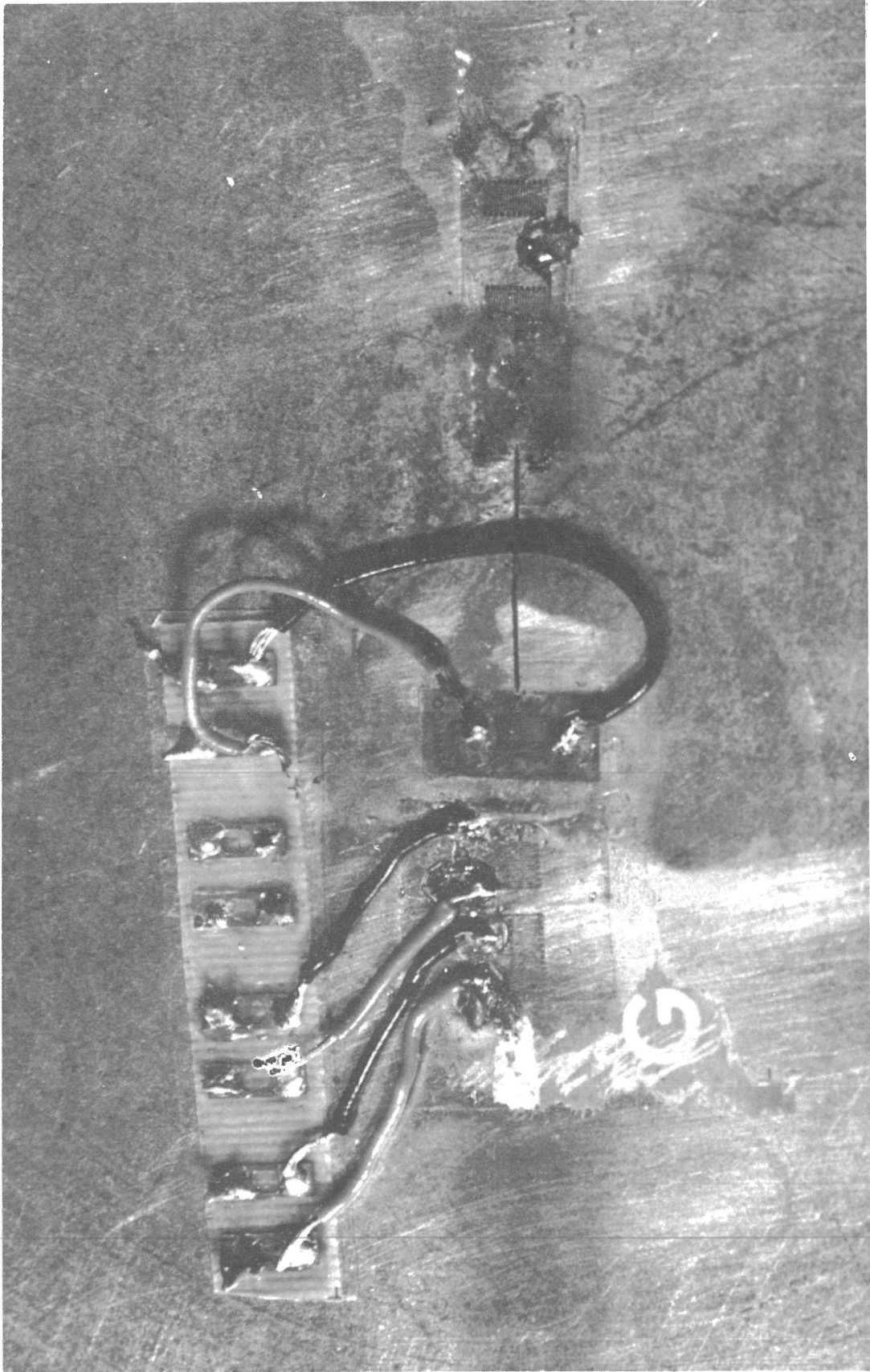


Fig. 7. Close-up of shell after testing (~3x)

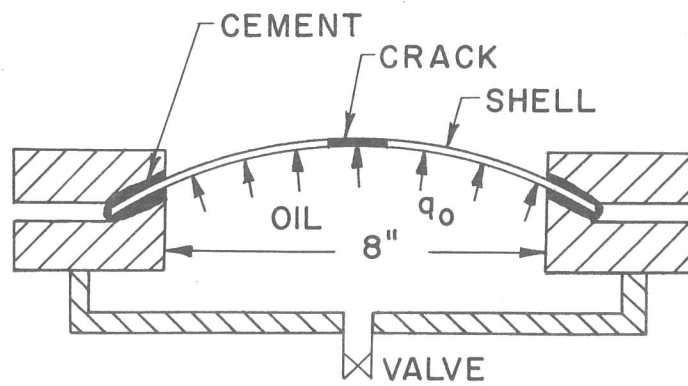


FIG. 8 - SCHEMATIC OF SHELL-RING ASSEMBLY

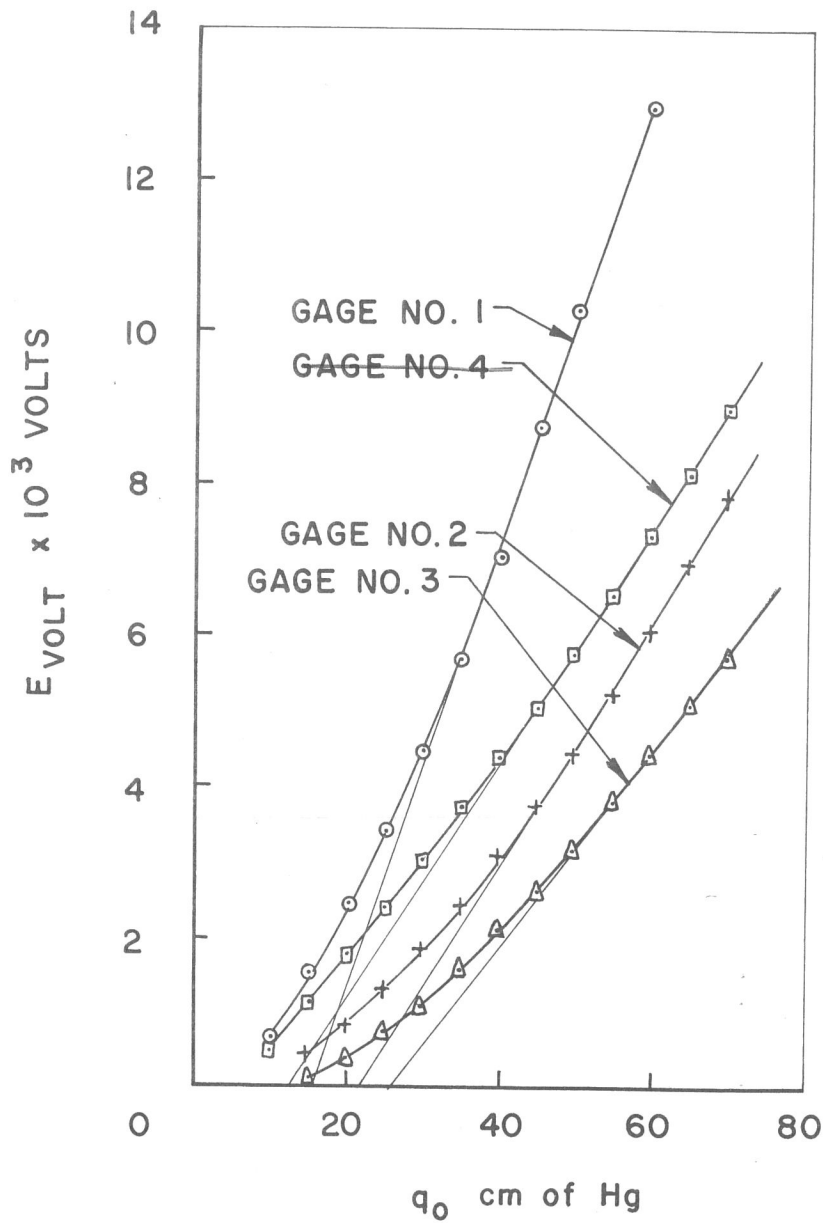
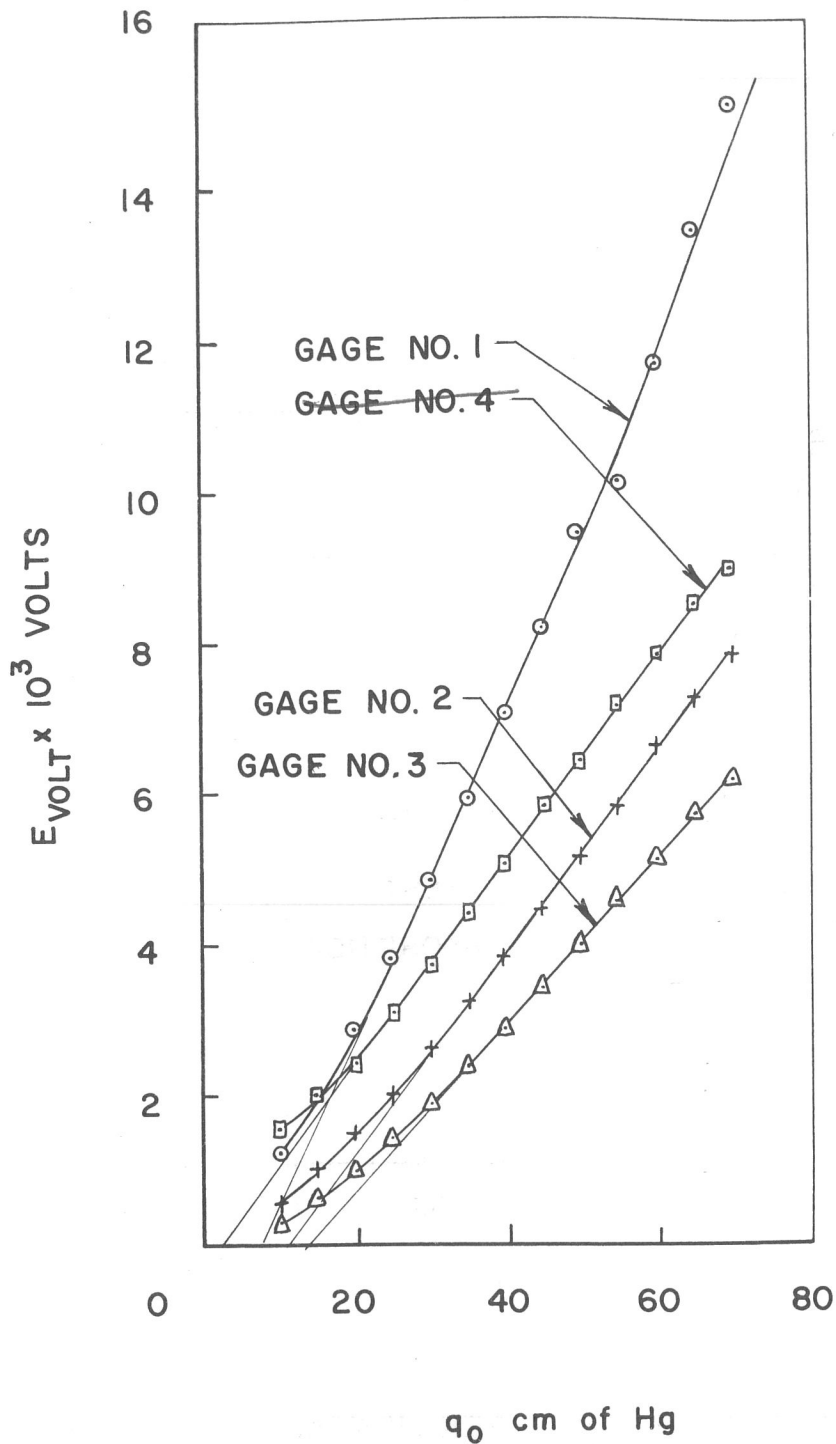


FIG. 9- TEST NO. 1. DATA FOR A CLAMPED SPHERICAL CAP CONTAINING A CRACK



omit gage 4.
I used this for E_x but I didn't use it for writing so omit.

FIG. 10 - TEST NO. 2 . DATA FOR A CLAMPED SPHERICAL CAP CONTAINING A CRACK

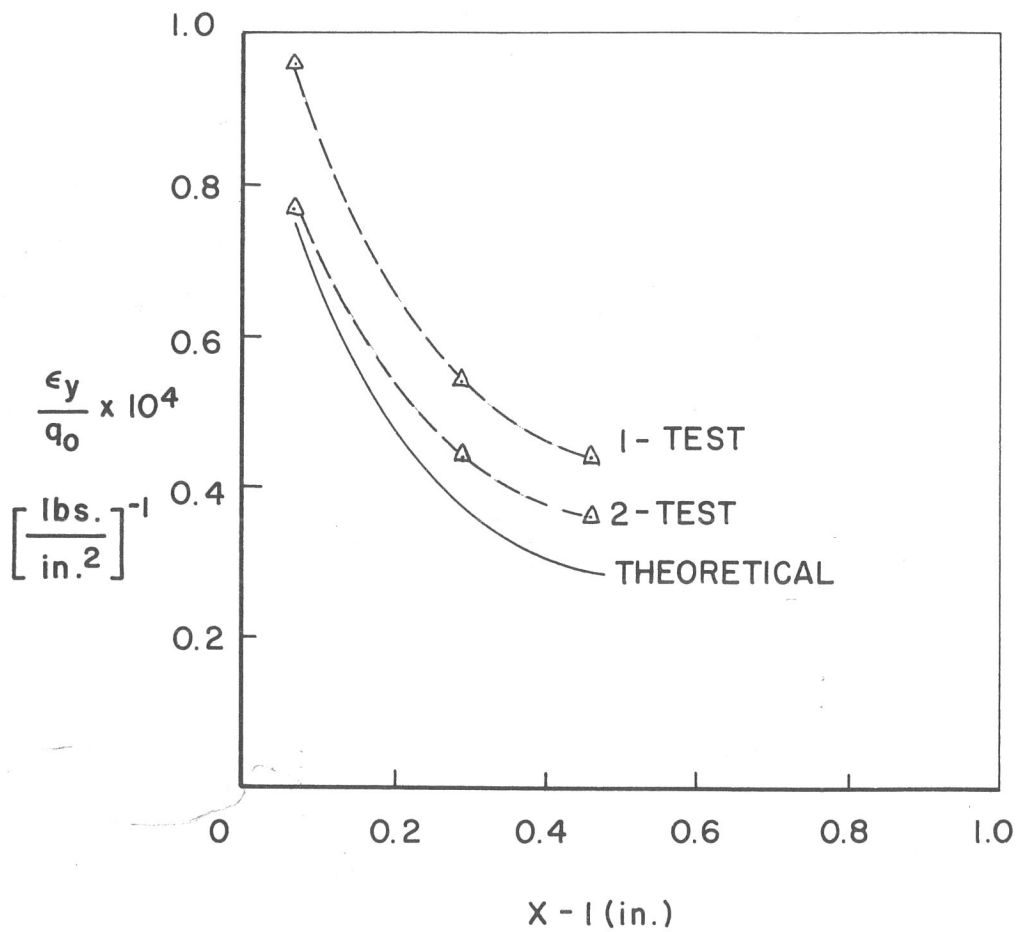


FIG. II - COMPARISON OF EXPERIMENTAL AND THEORETICAL STRAIN ALONG THE CRACK PROLONGATION FOR A CLAMPED SPHERICAL CAP SUBJECT TO INTERNAL PRESSURE q_0

NOTICES

When Government drawings, specifications, or other data are used for any purpose other than in connection with a definitely related Government procurement operation, the United States Government thereby incurs no responsibility nor any obligation whatsoever; and the fact that the Government may have formulated, furnished, or in any way supplied the said drawings, specifications, or other data, is not to be regarded by implication or otherwise as in any manner licensing the holder or any other person or corporation, or conveying any rights or permission to manufacture, use, or sell any patented invention that may in any way be related thereto.

- - - - -

Qualified requesters may obtain copies of this report from the Defense Documentation Center, (DDC), Cameron Station, Alexandria, Virginia.

- - - - -

DDC release to OTS not authorized

- - - - -

Copies of ARL Technical Documentary Reports should not be returned to Aerospace Research Laboratories unless return is required by security considerations, contractual obligations or notices on a specified document.